Data-constrained projections of methane fluxes in a Northern Minnesota Peatland in response to elevated CO_2 and warming

Shuang Ma[1], Jiang Jiang[2,3], Yuanyuan Huang[3,4], Zheng Shi[3], Rachel M. Wilson[5], Daniel Ricciuto[6], Stephen D. Sebestyen[7], Paul J. Hanson[6], Yiqi Luo[1, 8]

1, Center for Ecosystem Science and Society, Department of Biological Sciences, Northern Arizona University, Flagstaff, Arizona, USA

2, Department of Soil and Water Conservation, Nanjing Forestry University, Nanjing, Jiangsu, China

3, Department of Microbiology and Plant Biology, University of Oklahoma, Norman, Oklahoma, USA

4, Laboratoire des Sciences du Climat et de l'Environnement, 91191 Gif-sur-Yvette, France

5, Earth, Ocean and Atmospheric Sciences, Florida State University, Tallahassee, Florida, USA

6, Environmental Sciences Division and Climate Change Science Institute, Oak Ridge National Laboratory, Oak Ridge, Tennessee, USA

7, US Forest Service, Northern Research Station, Center for Research on Ecosystem Change, Grand Rapids, Minnesota, USA

8, Department of Earth System Science, Tsinghua University, Beijing, China

Corresponding author: Yiqi Luo (yiqi.luo@nau.edu)

Key points:

1. Using a data-model fusion approach, we constrained parameters and quantified uncertainties of CH_4 emission forecast.
2. Both warming and elevated air CO_2 concentrations have a stimulating effect on CH_4 emission.
3. The uncertainty in plant-mediated transportation and ebullition increased under warming.

Abstract: Large uncertainties exist in predicting responses of wetland methane (CH_4) fluxes to future climate change. However, sources of the uncertainty have not been clearly identified despite the fact that methane production and emission processes have been extensively explored. In this study, we took advantage of manual CH_4 flux measurements under ambient environment from 2011-2014 at the Spruce and Peatland Responses Under Changing Environments (SPRUCE) experimental site and developed a data-informed process-based methane module. The module was incorporated into the Terrestrial ECOsystem (TECO) model before its parameters were constrained with multiple years of methane flux data for forecasting CH_4 emission under five warming and two elevated CO_2 treatments at SPRUCE. We found that 9 ˚C warming treatments significantly increased methane emission by approximately 400%, and elevated CO_2 treatments stimulated methane emission by 10.4% - 23.6% in comparison with ambient conditions. The relative contribution of plant-mediated transport to methane emission decreased from 96% at the control to 92% at the 9 ˚C warming, largely to compensate for an increase in ebullition. The uncertainty in plant-mediated transportation and ebullition increased with warming and contributed to the overall changes of emissions uncertainties. At the same time, our modeling results indicated a significant increase in the emitted CH_4:CO_2 ratio. This result, together with the larger warming potential of CH_4, will lead to a strong positive feedback from terrestrial ecosystems to climate warming. The model-data fusion approach used in this study enabled parameter estimation and uncertainty quantification for forecasting methane fluxes.

Keywords

Data-model fusion, uncertainty, forecasting, methane, wetland, climate change

Plain Language Summary

Methane (CH_4) has 45 times the sustained-flux global warming potential of CO_2 over a 100-year scale, and it is directly responsible for approximately 20% of global warming since pre-industrial time. Wetlands are the single largest natural source of CH_4 emission and there is major concern about potential feedbacks between global climate change and CH_4 emissions from wetlands, as warming and atmospheric CO_2 are known to affect CH_4 emissions. However, extensive observed CH_4 flux data have not been well used to constrain model predictions of CH_4 emission in the future climate. Using a data-model fusion approach, we constrained parameters and quantified uncertainties of CH_4 emission forecast. We found both warming and elevated air CO_2 concentrations have a stimulating effect on CH_4 emission. The uncertainty in plant-mediated transportation and ebullition increased under warming.

1. Introduction

Methane (CH_4) is the simplest hydrocarbon produced by anaerobic microbes in the terminal step of organic matter remineralization. CH_4 has 45 times the sustained-flux global warming potential (SGWP) of CO_2 over a 100-year scale [*Neubauer and Megonigal*, 2015], and it is directly responsible for approximately 20% of global warming since pre-industrial periods [*Forster et al.*, 2007]. Wetlands are the single largest natural source of emitted CH_4 [*Bridgham et al.*, 2013] and there is major concern about potential feedbacks between global climate change and CH_4 emissions from wetlands, as warming and atmospheric CO_2 are known to affect CH_4 emissions [*Zhuang et al.*, 2004; *Bridgham et al.*, 2006]. However, extensive observed CH_4 flux data have not been well used to constrain model predictions of CH_4 emission in the future.

Process-based biogeochemistry models have been used to quantify global wetland CH_4 emissions with different complexities in model structures [*Cao et al.*, 1995; *Walter and Heimann*, 2000; *Zhang et al.*, 2002; *Zhuang et al.*, 2004; *Wania et al.*, 2010; *Riley et al.*, 2011; *Zhu et al.*, 2014]. However, large uncertainties exist in predicting responses of methane emissions to future climate change [*Frolking et al.*, 2006; *Bridgham et al.*, 2013]. In methane models, the uncertainties in model predictions stem from: 1) *Model structure* – process-based models with more details and controls are being developed at the site level and will be added into global models, but a bottleneck is the lack of spatially explicit physical, chemical and biological data [*Bridgham et al.*, 2013]; 2) *Parameter values* – some conceptual parameters used in methane models are not directly measurable and there is a limited variety of observational data do not comprehensively address various CH_4 emission pathways that are needed to constrain parameter values using data assimilation; and 3) *Forcing-data* [*Luo et al.*, 2015] – water table level and soil temperature are the two dominant controls on methane flux simulation because a) the water table position determines the extent of the catotelm zone where methane is largely produced (acrotelms may be

anoxic and methane may be produced in acrotelm) and the acrotelm where most methane is oxidized (methane can also be oxidized by methanotrophs in catotelm using Fe^{3+}, NO_3^-, SO_4^{2-}, etc. as electron accepters). [*Bartlett et al.*, 1990; *Dise and Gorham,* 1993; *Bubier et al.*, 1995; *Walter and Heimann*, 2000] and b) soil temperature affects the rates of microbiological processes such as fermentation, methanogenesis and methanotrophy [*Dise and Gorham,* 1993; *Frolking and Crill*, 1994; *Kettunen et al.*, 1999; *Walter and Heimann*, 2000].

Biogeochemical models and experimental results are generally consistent in showing that climate warming stimulates CH_4 emissions. Modeling results under +1 and +2°C warming scenarios found increases in CH_4 emission in northern wetlands by 17% and 11%, but decreases under higher elevated temperature due to the effect of soil moisture depletion [*Cao et al.*, 1998]. Short-term warming and coupled water table level × warming *in situ* or mesocosm manipulations have been used at the site level to explore the responses of northern peatland CH_4 emission to climate warming from +0.6 to +2.0 °C. These studies found warming increased CH_4 fluxes by 15%-550% or had no effect based on the condition of water table variation and vegetation change [*Verville et al.*, 1998; *Granberg et al.*, 2001; *Updegraff et al.*, 2001; *Turetsky et al.*, 2008]. However, these studies only warmed the soil surface , which may have precluded deep soil responses to warming especially in northern wetlands where a significant fraction of C is stored in deep peat layers. Nevertheless, methane fluxes measured under warming or elevated CO_2 (eCO_2) have never been incorporated into models via data-model fusion or used to constrain models in projecting methane emission under climate change.

Net methane emission includes contributions from plant-mediated transport, diffusion and ebullition (i.e. bubble release). Over 90% of the methane emission in a *Carex*-dominated fen near Schefferville, Quebec, Canada was mediated by plants [*Whiting and Chanton*, 1992]. Emergent

plants in a peatland in southern Michigan, USA accounted for 64% - 90% of the net CH_4 efflux in plant enclosure experiments [*Shannon et al.*, 1996]. Plant-mediated fluxes averaged 69.8 ± 11.8 mg CH_4 m^{-2} d^{-1} and accounted for *ca.* 50% of total fluxes at the Alaska Peatland Experiment site [*Shea et al.*, 2010]. In the same study, diffusion contributed to less than 9% of total CH_4 flux (up to 7.6 mg CH_4 m^{-2} d^{-1}) and ebullition accounted for *ca.* 41% of total CH_4 flux. However, the quantity and temporal-spatial scales of experimental studies are limited, so the responses of the relative contributions of the three processes to climate warming have not been unraveled either using experiments or modeling approaches.

In process-based methane models, the individual pathway of CH_4 emission is related to CH_4 pool size (CH_4 concentration), which is primarily determined by CH_4 production. Once the parameters in CH_4 production, plant-mediated transportation, ebullition, and diffusion are constrained by observed data and the prior range of parameter values with a data-model fusion technique [*Wang et al.*, 2009; *Richardson et al.*, 2010; *Keenan et al.*, 2011, 2012; *Smith et al.*, 2013], the simulation of differential contributions from the three pathways under warming and eCO_2 may be improved. The Spruce and Peatland Responses Under Changing Environments (SPRUCE) experimental site is unique in coupling deep peat heating (to a depth of 2 m) and above-ground warming at +0°C, +2.25°C, +4.5°C, +6.75°C and +9 °C above ambient temperature along with eCO_2 treatment [*Hanson et al.*, 2016a]. Although not enough data are yet available for validating methane emission under warming treatments, the extensive data sets released or coming out from SPRUCE will enable parameter estimation, uncertainty quantification, and contribution from each pathway to better forecast methane fluxes under warming and eCO_2.

In this study, we focus on developing a data-informed process-based model using the methane chamber measurement data from a northern peatland in northern Minnesota where the SPRUCE

project is occurring. We also looked at differential responses of CH_4 production, oxidation, diffusion, ebullition and plant-mediated transportation to warming and eCO_2. We hypothesized that both warming and eCO_2 would increase methane emission in this ombrotrophic bog, with differential responses of each process due to the differential temperature dependencies of methanogenesis and respiration.

2. Methods

2.1 Site Description and treatments

We took Spruce and Peatland Responses Under Climatic and Environmental Change experiment (SPRUCE) as our case study site. The SPRUCE project is conducted to study the responses of northern peatland to climate warming (+0, +2.25, +4.5, +6.75, +9 °C) and elevated atmospheric CO_2 concentration (+0 and +500 ppm) [*Hanson et al.*, 2016a]. The SPRUCE experiment is located in the 8-ha S1 bog that has been at the Marcell Experimental Forest (MEF, N 47° 30.476' W 93° 27.162', 418 m above mean sea level), a site in northern Minnesota, USA, with a long-term research program that is administered by the USDA Forest Service. Temperature and precipitation have been measured since 1961 at the MEF South Meteorological station, which is about 1 km from the SPRUCE experiment. The mean annual temperature from 1961 to 2009 was 3.4 °C, and the mean annual precipitation was 780mm [*Sebestyen et al.*, 2011b]. Mean annual air temperatures have increased approximately 0.4 °C per decade over the last 50 years [*Sebestyen et al.*, 2011b]. Vegetation within the S1 bog is dominated by trees species *Picea mariana* and *Larix laricina*, a variety of ericaceous shrubs, and *Sphagnum* sp. moss. The bog also has graminoids *Carex trisperma* and *Eriophorum spissum*, as well as forbs *Sarracenia purpurea* and *Smilacina trifolia*. Mean peat depth in this bog is around 2-3m [*Parsekian et al.*, 2012].

The water table typically fluctuates within the top 30 cm of peat at five long-studied bogs on the MEF [*Sebestyen et al.*, 2011a]. Within SPRUCE, water table levels have been measured half hourly (except during freezing temperatures) at the meteorological station EM1 on the southwest side of the experiment site since Jan 2011. The sensor was placed in a hollow (microtopographic lows that are interspersed among hummocks of bogs [*Verry*, 1984]). A TruTrack WT-VO water level sensor was used to measure water table levels that were logged with a Campbell Scientific

155 CR1000 data logger. In this study, water table height is expressed as zero at the hollow surface
156 during late spring or early summer [*Sebestyen and Griffiths*, 2016]. Community-level CH_4
157 emission were measured once each month during snow-free months beginning during 2011 using
158 a portable open-path analyzer in each plot at "large collars" (area of 1.13 m^2) that have been
159 previously described [*Hanson et al.*, 2016b; *Hanson et al.*, 2017]. Mean annual air temperature at
160 2 meters height ranged 1.91-5.10 ℃, mean annual soil temperature at 30 cm depth ranged 5.83-
161 7.06 ℃, annual precipitation ranged 651-717 mm during the year 2011-2016. In total, 45 daily
162 CH_4 chamber measurement data points were integrated from ambient plots from 2011-2016. We
163 took the mean value if there is more than one plot that have data on the same date, variations in
164 different ambient plots were not simulated due to our purpose to represent the site level CH_4
165 emission.

166 **2.2 Model description and key processes**

167 **2.2.1 Overview of TECO**

168 The process-based biogeochemistry model, TECO (Terrestrial ECOsystem model), simulates
169 carbon, nitrogen and hydrology cycles in terrestrial ecosystems [*Weng and Luo*, 2008]. The model
170 has four major components: canopy photosynthesis, soil water dynamics, plant growth (allocation
171 and phenology), and soil carbon and nitrogen transfers. A detailed description of TECO is
172 available in *Weng and Luo* [2008] and *Shi et al.* [2015b]. The canopy sub-module was mainly
173 derived from Wang and Leuning's [1998] two-leaf model, which simulated processes of canopy
174 photosynthesis, conductance, energy balance, and transpiration. The soil water dynamics sub-
175 module has ten soil layers and simulates soil moisture dynamics based on precipitation,
176 evapotranspiration and runoff. Evaporation is regulated by the first soil layer water content and the
177 evaporative demand of the atmosphere. Transpiration is determined by stomatal conductance and

178 the soil water content of layers where roots are present. When precipitation exceeds water recharge
179 to soil water holding capacity, runoff occurs. The C transfer sub-module simulates movement of
180 C from plants to three soil C pools through litter fall and the decomposition of litter and soil organic
181 C. Carbon fluxes from litter and soil carbon pools are based on residence time of each C pool and
182 the C pool sizes [*Luo and Reynolds*, 1999].
183 The TECO model has been adapted to the SPRUCE site by *Jiang et al.* [2017] and *Huang et al.*
184 [2017] to study the forecasting uncertainty in terrestrial carbon cycles and soil thermal dynamics.
185 Five out of 18 parameters related to photosynthesis, respiration, plant growth and C turnover were
186 constrained by 11 pretreatment data sets from 2011 to 2014 [*Jiang et al.,* 2017]. Since water table
187 is an important variable determining aerobic and anaerobic belowground environments and further
188 influence CH_4 production, oxidation and diffusion, we improved the model by incorporating
189 hourly time step water table dynamics and methane production, oxidation, diffusion, ebullition and
190 plant-aided transportation processes into the model. We followed the original TECO_SPRUCE
191 structure and divided the soil into 10 layers, with first five layers that were 10-cm thick and other
192 five layers that were 20-cm thick. (most peatland roots are distributed in the top 60 cm peat layer).
193 The conceptual structure of water table and methane flux models and the incorporation into
194 TECO_SPRUCE are shown in Fig.1 and further described below.
195 **2.2.2 Water table module**
196 New algorithms were developed and integrated into the hydrological part of TECO to estimate the
197 water table level and the influence of the water table on soil moisture in the unsaturated zone.
198 Generally, the water table module followed Granberg's [*Granberg et al.*, 1999] method and this
199 approach has been widely applied in global methane models [*Zhuang et al.*, 2004; *Wania et al.*,
200 2009a; *Zhu et al.*, 2014]. Based on our observation data, these bog soils are always saturated below

30cm [*Tfaily et al.*, 2014], except during some extreme droughts [*Sebestyen et al*., 2011]. Therefore, we set 30cm as the maximum water table depth (z_b). The system was considered as a simple bucket model. The changes in water content of the top 30 cm soil profile can be calculated by a water balance model characterized by water input and output at hourly time step. The level of the water table is determined by soil moisture change. We used a constructed function for water-holding capacity to simulate the dynamics of the water table level. In the unsaturated zone, we use a quadratic function and the soil volumetric water content (θ_{us}) increases from the vegetation surface volumetric water content (θ_s) to the position of the water table (z_{wt}) as follows:

$$\theta_{us}(z) = \min\left[\varphi, \theta_s + (\varphi - \theta_s)\left(\frac{z}{z_{wt}}\right)^2\right], \quad (1)$$

where φ has a constant value of 0.95, z is the depth in soil (mm), and θ_s is adapted from Hayward and Clymo [1982] and represented as:

$$\theta_s = max\left[\theta_{smin}, \varphi - (a_z z_{wt})\right], \quad (2)$$

where θ_{smin} is the minimum volumetric water content still held by capitulum of *Sphagnum* at the soil surface and set to 0.25, a_z is the linearly decreasing gradient given by:

$$\mathrm{a_z} = \frac{\varphi - \theta_{smin}}{z_{\theta smin}}, \quad (3)$$

where $z_{\theta smin}$ is the maximum suction interval given the value 100 mm. Thus, the total volume of water in soil profile above z_b would be:

$$V_{tot} = \varphi(z_b - z_{wt}) + \int_0^{zwt} \theta_{us}(z)\, dz, \quad (4)$$

where the first part of the equation represents the water content in the saturated zone above z_b, and the second part of the equation refers to the water content in the unsaturated zone. If the whole

profile is saturated, the height of standing water is represented by the difference of V_{tot} and $z_b\varphi$. The final equation for water table depth is:

$$z_{wt} = \begin{cases} \sqrt{\frac{3(\varphi z_b - V_{tot})}{2a_z}} & if\ z_{wt} > 0\ and\ z_{wt} \le z_{\theta smin} \\ \frac{3(\varphi z_b - V_{tot})}{2(\varphi - \theta_{smin})} & if\ z_{wt} > z_{\theta smin}\ and\ z_{wt} < z_b \\ -(V_{tot} - z_b\varphi) & if\ z_{wt} < 0 \end{cases}, \quad (5)$$

where a positive value of z_{wt} indicates the water table is below the hollow surface, and a negative value of z_{wt} indicates the water table is above the hollow surface.

2.2.3 Methane module

TECO_SPRUCE_ME explicitly considers the transient and vertical dynamics of CH_4 production (P_{ro}, methanogenesis), CH_4 oxidation (O_{xi}, methanotrophy) and CH_4 transport from the soil to the atmosphere which includes ebullition (E_{bu}), diffusion (D_{ifu}), and plant-mediated transport (A_{ere}) in the soil profiles. The structure and processes were adapted from a number of previous studies and models [*Walter and Heimann*, 2000; *Zhuang et al.*, 2004; *Wania et al.*, 2010; *Riley et al.*, 2011]. We assume that soils can be separated in to an unsaturated zone above the water table and a saturated zone below the water table. Methane oxidation occurs in the unsaturated zone and rhizosphere (as explained in Section 2.2.3.4), methane production occurs in the saturated zone [*Walter and Heimann*, 2000; *Zhuang et al.*, 2004; *Zhu et al.*, 2014; *Cao et al.*, 1996]. To simulate methane dynamics within the soil, we divided the soil column into 10 layers, with first five layers that were 10-cm thick and other five layers that were 20-cm thick. Within each soil layer, CH_4 concentration dynamics were calculated by a transient reaction equation:

$$\frac{\partial([CH_4])}{\partial t} = P_{ro}(z,t) - O_{xi}(z,t) - E_{bu}(z,t) - A_{ere}(z,t) - \frac{\partial D_{ifu}(z,t)}{\partial z}\ , \quad (6)$$

where [CH_4] is soil CH_4 concentration (g C m^{-3}), z is the depth in soil (mm), t is time step (hr), $P_{ro}(z,t)$ is the CH_4 production rate, $O_{xi}(z,t)$ is the CH_4 oxidation rate, $E_{bu}(z,t)$ is the ebullitive CH_4 emission rate, and $A_{ere}(z,t)$ is the plant-mediated transportation rate. The term $\frac{\partial D_{ifu}(z,t)}{\partial z}$ is the flux divergence resulting from the diffusion of methane into/out of soil layer z from the lower/upper soil layer or the atmosphere (for the first layer). A negative value indicates a reverse transfer direction determined by the difference of CH_4 concentration between adjacent layers. The total emission of CH_4 from soil to atmosphere ($F_{CH_4}(t)$) is represented as:

$$F_{CH_4}(t) = E_{bu}(t) + A_{ere}(t) + D_0(t), \quad (7)$$

where within each time step, $E_{bu}(t)$ is the sum of all the ebullitive CH_4 emissions in soil layers, $A_{ere}(t)$ is the sum of all the plant-aided CH_4 emissions in soil layers, and $D_0(t)$ is the diffused flux from the first soil layer into the atmosphere (a negative value indicates diffused flux from the atmosphere into the soil).

2.2.3.1 Methane production

Methanogenesis is the terminal step of soil organic carbon decomposition under anaerobic conditions [*Conrad*, 1999]. This process is determined by carbon substrate supply and soil environmental conditions such as water table via O_2 availability and soil temperature [*Walter and Heimann*, 2000]. In TECO_SPRUCE_ME, CH_4 production occurs only in the saturated zone of the soil profile. Similar to CLM4Me [*Riley et al.*, 2011], LPJ-WHyMe [*Wania et al.*, 2010; *Spahni et al.*, 2011] and TRIPLEX-GHG [*Zhu et al.*, 2014] models, we assume there are no time delays between fermentation and methanogenesis so that CH_4 production within the catotelm is directly related to heterotrophic respiration from soil and litter (R_h, g C $m^{-2} h^{-1}$):

$$P_{ro}(z,t) = R_h(z,t)\, r_{\_me} f_{stp}(z,t) f_{pH} f_{red}\,, \quad (8)$$

where $R_h(z,t)$ is redistributed in different soil layers by assuming that 50% is associated with roots and the rest is evenly distributed among the top 0.3 m of soil [*Riley et al.*, 2011]. The distribution of root biomass was estimated from minirhizotrons and root in-growth cores over the summer of 2013 [*Iversen et al.*, 2017]. The fractions of root biomass in each soil layer ($f_{root}(z)$) were estimated as 0.1, 0.25, 0.25, 0.2, 0.1, 0.05, 0.025, 0.015, 0.005, and 0.005 from the upper boundary (the soil surface or water surface if the water table is above the soil surface) to a lower boundary. The parameter $r_{\_me}$ is the potential ratio of anaerobically mineralized C released as CH_4, which is an ecosystem specific conversion scaler. The soil environmental scalers, f_{stp}, f_{pH}, and f_{red} are for soil temperature, pH and redox potential. The factor f_{stp} is a multiplier enhancing CH_4 production with increasing soil temperature. It uses a Q_{10} function with a Q_{10} coefficient for production (Q_{10pro}), a highest temperature (T_{max}) and optimum temperature (T_{opt}) for CH_4 production. We used Q_{10pro} which refers to a parameter that describes the temperature sensitivity of the reaction from CO_2 to CH_4. Q_{10Rh} describes temperature sensitivity of the reaction from soil organic carbon to CO_2, which has already been adapted and constrained by *Jiang et al.* [2017]. Previous studies have shown that in winter when soil temperature is below 0 ℃, the methanogenesis rate is significantly lower than that of rates observed during growing seasons [*Whalen and Reeburgh*, 1992; *Shannon and White*, 1994]. Therefore, CH_4 production in the model only occurs when soil temperature is above 0 ℃ and below an extremely high temperature of 45 ℃ as shown below:

$$f_{stp}(t) = \begin{cases} 0 & if\ T_{soil} < 0 \\ Q_{10}^{\frac{T_{soil}(t) - T_{optpro}}{10}}_{pro} & if\ 0 \le T_{soil} \le T_{max} \\ 0 & if\ T_{soil} > T_{max} \end{cases}, \quad (9)$$

where $T_{soil}(t)$ is the hourly soil temperature, and T_{optpro} is the optimum temperature for CH_4 production, which varies across ecosystems. In this study we chose an value of 20 ℃ since this was the maximum temperature for which methane production was examined in incubations of peat from this site [*Wilson et al.*, 2016].

The factors f_{pH} and f_{red} are nominally set to a constant value of 1.0 due to the model sensitivity [*Riley et al.*, 2011; *Meng et al.*, 2012] and uncertainty in characterizing these two parameters [*Whalen, 2005*, *Le Mer and Roger,* 2001; *Wania et al.*, 2010]. In the CLM4Me model, the effect of pH and redox potential on net fluxes were tested in the sensitivity analysis, and resulted in less than a 20% change in net CH4 emission at high latitudes [*Riley et al.*, 2011]. Redox potential does not have substantial impacts on methane emissions at seven wetland sites including one adjacent to the Marcell Experimental Forest in north central Minnesota [*Meng et al.,* 2012; *Shurpali and Verma*, 1998]. *Wania et al.* [2010] argued that the pH and redox factors are so poorly characterized that they should be excluded. Many of the current process-based methane models use a single value for the pH scaler calculated from the soil property that does not change with time and depth. In many process-based methane models a step function is used for calculating the redox potential scaler [*Fiedler and Sommer*, 2000; *Segers and Kengen* 1998; *Zhang et al.*, 2002], which is decided by root distribution, fraction of water filled pore space, the water table position, as well as several other constant parameters with a single value across different ecosystems such as change rate of soil redox potential under saturated conditions, cross-sectional area of a typical fine root and fine root length density. In our model, the potential ratio of anaerobically mineralized C released as CH_4 can reflect some of the information on the effects of pH and redox potential to methane production. We kept f_{pH}, and f_{red} in equation (8) because as more information become available we might be able to improve their calculation in our later versions.

2.2.3.2 Methane oxidation

Methane is oxidized by methanotrophs in both the acrotelm (O_2 as electron accepter) and the catotelm (Fe^{3+}, NO_3^-, SO_4^{2-}, etc. as electron accepters). Like in other methane models [*Cao et al.*, 1996; *Zhuang et al.*, 2004], we only consider CH_4 oxidation in the acrotelm and during the process of plant-mediated transportation (as explained in Section 2.2.3.4). Given that CH_4 oxidation is largely controlled by CH_4 concentration, it is assumed to follow the Michaelis-Menten kinetics [*Bender and Conrad*, 1992] represented by:

$$O_{xi}(z,t) = \mathrm{O}_{\max} f_{CH4}(z,t) f_{sto}(z,t), \quad (10)$$

where $\mathrm{O}_{\max}$ is the ecosystem-specific maximum oxidation rate (μmol L^{-1} h^{-1}) for CH_4, f_{CH4} is the CH_4 concentration coefficient equal to: $\frac{[CH_4](z,t)}{K_{CH4} + [CH_4](z,t)}$, where $[CH_4]$ denotes the soil methane concentration (g C m^{-3}) at time t and depth z, and K_{CH4} is Michaelis constant. $f_{sto}(z,t)$ is an environmental scaler associated with a Q_{10} function, with Q_{10oxi} and ecosystem-specific optimum temperature for oxidation (T_{optoxi}).

2.2.3.3 Aqueous and gaseous diffusion

In process based models, CH_4 emission from the soil to the atmosphere is represented by three pathways: diffusion ($D_{if}(z,t)$), plant-mediated transport ($A_{ere}(z,t)$), and ebullition ($E_{bu}(z,t)$).

The CH_4 diffusion across soil layers follows Fick's first law,

$$D_{ifu}(z,t) = D_{CH_4}(z,t) \frac{\partial [CH_4](z,t)}{\partial_z}, \quad (11)$$

where $D_{ifu}(z,t)$ is the diffusive flux at depth z (mm) and time t (hour), and $[CH4](z,t)$ is the corresponding methane concentration (g C m^{-3}). The diffusion coefficient ($D_{CH_4}(z,t)$) varies with soil layers, the calculation is adapted and modified from *Walter and Heimann* [2000] :

$$D_{coe}(z,t) = \frac{(f_{air}(z,t))^{10/3}}{\varphi^2} \times D_{CH4a}\,, \quad (12)$$

$$D_{CH_4}(z,t) = \begin{cases} D_{CH_{4W}}, & f_{air}(z,t) \le 0.05, \\ D_{coe}(z,t), & f_{air}(z,t) > 0.05. \end{cases} \quad (13)$$

where $D_{coe}(z,t)$ is the CH_4 diffusivity in soil; D_{CH4a} and D_{CH4w} are the diffusion coefficient of methane in bulk air ($0.2\ cm^2 s^{-1}$) and in water ($0.2 \cdot 10^{-4}\ cm^2 s^{-1}$) [*Walter and Heimann*, 2000]; φ is soil porosity; f_{water} is the fraction of water-filled pore space in soil calculated from soil water content; and f_{air} is the fraction of air-filled pore space in soil calculated by $\varphi - f_{water}$. Only the net emission or uptake from first layer ($D_0(t)$) directly contributes to the final CH_4 flux exchange between soil and the atmosphere. For boundary conditions, the methane flux at the bottom boundary was set to zero. The atmospheric CH_4 concentration at the soil surface (or water surface if the water table is at or above the soil surface) is set to 0.076 μM. At the water-air interface the methane concentrations in both phases are assumed to be in equilibrium. For layers where air fraction ($f_{air}(z,t)$) < 0.05, the diffusivities for water were used. When $f_{air}(z,t)$ > 0.05, the diffusivities in soil were used.

2.2.3.4 Plant-mediated transportation

Vascular plants enhance CH_4 emissions by transporting CH_4 from the point of methanogenesis in the rhizosphere directly to the atmosphere [*Joabsson et al.*, 1999]. When gas is transported through intercellular spaces (molecular diffusion) or aerenchyma tissues, methane emissions are larger than through diffusion alone. Because the diffusive CH_4 flux may bypass the soil profiles where it might otherwise be consumed above water table level by oxygen (O_2) or below the interface by Fe^{3+}, NO_3^-, SO_4^{2-}, etc. [*Chanton and Dacey*, 1991]. Conversely, plants could reduce CH_4 emissions by releasing O_2 to the rhizosphere thereby enhancing CH_4 oxidation. In TECO_SPRUCE_ME, plant-

mediated transport is adapted from Walter's model [*Walter and Heimann*, 2000]. We described two processes: CH_4 transported through plants and directly into the atmosphere (the 'chimney effect') and enhanced CH_4 oxidation during upward transport in tissues. Briefly, it is modeled as a function of the vegetation condition (T_{veg}), the fraction of root biomass in each soil layer ($f_{root}(z)$), the growing state of plants ($f_{growth}(t)$), the fraction of CH_4 consumed by oxidation in rhizosphere (P_{ox}) and the distribution of soil CH_4 concentrations in the soil:

$$A_{ere}(t) = k_{pla} T_{veg} f_{root}(z) f_{growth}(t) \left[CH_4\right](1 - P_{ox}), \quad (14)$$

where k_{pla} is a rate constant with the unit 0.01 h^{-1}; The parameter T_{veg} is a factor of transport ability at the plant community level, which is set by species composition and plant density; The fraction of CH_4 consumed by oxidation in rhizosphere, P_{ox}, is set to 50%, although there is high variability of observed values [*Gerard and Chanton*, 1993; *Schipper and Reddy*, 1996]. The multiplier $f_{growth}(t)$ describes the effects of the growing stage of vegetation on plant-mediated methane transport [*Walter and Heimann,* 2000; *Zhuang et al.,* 2004], it is determined by leaf area index (LAI) and soil temperatures (Tsoil),

$$f_{growth}(t) = \begin{cases} LAI_{min} & if\ T_{soil} < T_{gr} \\ LAI_{min} + LAI_{max}\left(1 - \left(\frac{T_{mat} - T_{soil}}{T_{mai} - T_{gr}}\right)^2\right) & if\ T_{gr} \le T_{soil} \le T_{mat} \\ LAI_{max} & if\ T_{mat} > T_{soil} \end{cases}, \quad (15)$$

where LAI_{min} is the minimum LAI associated with the beginning of plant growth; while LAI_{max} is the maximum LAI associated with plant at maturity; We used T_{gr} as the temperature at which plants starts to grow; and T_{mat} is the temperature at which plants reach maturity. Similar to *Walter and Heimann* [2000] and *Zhuang et al.* [2004], LAI_{min} and LAI_{max} were chosen to be 0 and 4, respectively; T_{gr} is equal to 7°C where the annual mean soil temperature is above 5°C, otherwise,

T_{gr} is equal to 2°C. The annual mean soil temperature at our study site is 5.83-7.06°C, so the value 7°C was used. T_{mat} is assumed to equal T_{gr} + 10°C.

A range of 0-15 for T_{veg} was used in a process based model at five wetland sites [*Walter and Heimann*, 2000]. In Zhuang *et al.*[2004], the value of T_{veg} was given as 0.5 for tundra ecosystems and 0.0 for boreal forests, as they considered trees to not contribute to plant-mediated transport; shrubs to mediate some gas transportation; and grasses, ferns, and sedges to be good mediators of gas transport. The assignments of this parameter are empirical and would be improper for trees and shrubs that mediate CH_4 transportation. In our study we give a 0-15 range for T_{veg} from those studies and try to constrain the value by using data assimilation as illustrated below.

2.2.3.5 Ebullition

We assumed that bubbles form when the CH_4 concentration exceeded a certain threshold ($[CH_4]_{thre}$=750 μmol L^{-1}) [*Walter and Heimann*, 2000] and that bubbles were directly emitted into the atmosphere when the water table was above the soil surface. Otherwise, the bubbles are added to the soil layer just above the water table and then continue to diffuse through the soil layers if z is below the water level:

$$E_{bu}(z,t) = \begin{cases} K_{ebu}([CH_4](z,t) - [CH_4]_{thre}) & if\ [CH_4] > [CH_4]_{thre} \\ 0.0 & if\ [CH_4] \le [CH_4]_{thre} \end{cases}, \qquad (15)$$

where K_{ebu} is a rate constant of 1.0 h^{-1} [*Walter and Heimann*, 2000]. No bubbles are formed if z is above the water level.

2.3 Sensitivity test for data assimilation

The efficiency of data assimilation is affected by the number of observational data sets as well as the amount of data in each set. In this study, methane emission data is the only available observational data set for data assimilation. Therefore, we chose only the most sensitive parameters

for data assimilation because the observational variable is usually sensitive to the changes in parameter values when a parameter can be constrained by that variable in data assimilation [*Roulier and Jarvis*, 2003]. We chose nine key parameters used in TECO_SPRUCE_ME (Table 1) for the initial sensitivity test, and most of the remaining parameters are physical constants. The sensitivity of parameters are determined by sensitivity index (*I*) defined as:

$$\mathrm{I} = \frac{(y_2 - y_1)/y_0}{2\Delta x/x_0} \quad , \tag{16}$$

where y_0 is the model output (methane emission) with an initial value of the independent variable x_0 (parameters in Table 1). The independent variable value varied by $\pm \Delta$x with corresponding dependent variable values y_2 and y_1. Δx was set at 0.25 times of initial values. The sensitivity index (*I*) was used by *Lenhart et al*. [2002] and *Zhu et al.* [2014] to quantify sensitivity, which was ranked into four levels, the grading of the index could be found in *Lenhart et al.* [2002].

2.4 Data Assimilation

Using the Bayesian probabilistic inversion technique, we estimated the posterior distribution of model parameters based on prior knowledge of parameter ranges (Table 1) and field chamber measurements of CH_4 emissions. Since the whole-ecosystem warming (air heating and deep peat heating) treatments were recently initiated on August 12, 2015 [*Hanson et al.*, 2017], and the number of whole-ecosystem warming treatment data points were not enough for data assimilation, we only compiled chamber measurement data in ambient plots from 2011-2014 for data assimilation and 2015-2016 for validation. Both the observed data and simulated results were rescaled to a daily emission unit for comparison. In order to project future methane flux uncertainty only related to parameter values, we conducted 100 forecasting runs by randomly choosing parameter sets from their posterior distributions, we randomly picked one set of stochastically generated environmental variables and used the same set for all the forecasting runs.

412 Bayes' theorem provides an equation in which the posterior probability density function $p(\theta \mid Z)$
413 of model parameters for given observations Z is based on prior knowledge of parameter
414 distribution $p(\theta)$ and the likelihood function $p(Z \mid \theta)$:

415 $$p(\theta \mid Z) \propto p(Z \mid \theta) p(\theta) \tag{17}$$

416 Here we assume the prior knowledge of parameter distribution $p(\theta)$ is uniformly distributed. Due
417 to the equifinality and unidentifiable parameters when using only one observation data stream to
418 constrain multiple parameters [*Luo et al.*, 2009], we only chose 4 parameters with high sensitivity
419 to run data assimilation and the prior ranges were cited from published papers for the same or
420 similar ecosystems (Table1). The errors between each observation data and model simulation
421 result independently follow normal distribution with a zero mean, so the likelihood function is
422 represented by:

423 $$p(Z \mid \theta) \propto exp\left\{ - \sum_{t \in Z_i} \frac{[Z_i(t) - X(t)]^2}{2\sigma_i^2(t)} \right\} \tag{18}$$

424 where $Z_i(t)$ is the only observation stream at time t, $X(t)$ is the simulated corresponding variable,
425 and $\sigma_i(t)$ is the standard deviation of observation set.

426 The Markov chain Monte Carlo (MCMC) technique was used for posterior probability distribution
427 of parameters sampling with adaptive Metropolis-Hastings (M-H) algorithm. A new vector of
428 candidate parameters was repeatedly proposed based on the accepted parameters in the previous
429 steps by a normal distribution. The new set of parameter values would be accepted either by
430 reducing the sum of standard deviation from observation and model, or being randomly accepted
431 with a probability of 0.05. Detailed information on sampling posterior distribution is well
432 illustrated in *Jiang et al*. [2017]. We ran 4 chains of 50,000 simulations with an acceptance rate
433 around 30%, and used the Gelman-Rubin statistic [*Gelman and Rubin*, 1992; *Xu et al.*, 2006] to

434 check the convergence of sampling chains. Only the second half of accepted parameter values
435 were used for posterior analysis considering the burn-in period in the first half.

436 **2.5 Stochastic Weather Generation**

437 We generated three hundred sets of 10-year environmental variables (2016-2024). Daily air
438 temperature and precipitation were stochastically generated based on historical data from 1961-
439 2014 at the MEF South Meteorological station using a vector autoregressive model (VAR, Fig. 2).
440 To match the model time step, hourly precipitation was obtained by evenly distributing daily
441 precipitation for each hour, hourly air temperature was interpolated from daily maximum and
442 minimum, and soil temperature was calculated from air temperature based on linear regression
443 between soil temperature and air temperature at S1 Bog from 2011-2014. The generated air
444 temperature generally follows the same distribution as the historical temperature (Fig. 2a). The
445 standard deviation of generated temperature decreases with increasing daily mean temperature
446 (Fig. 2c), which indicates a larger uncertainty of generated future temperature in winter than in
447 summer. Future prediction of precipitation is similar to the historical precipitation with slightly
448 higher variation (Fig. 2bd). More details on stochastic weather generation process and the
449 assignment of environmental forces can be found in *Jiang et al*. [2017]. We increased both the air
450 temperature and soil temperature by 2.25 ˚C, 4.5 ˚C, 6.75 ˚C, 9 ˚C and the atmospheric CO_2 value
451 by 500 ppm to simulate CH_4 emission in different scenarios manipulated at the SPRUCE site.

3. Results

3.1 Parameters constrained by data assimilation in TECO_SPRUCE_ME

The model output was sensitive to 5 out of 9 tested parameters in the growing season (Fig. 3): potential ratio of anaerobically mineralized carbon released as CH_4 ($r_{\_me}$), Q_{10} for CH_4 production (Q_{10_pro}), maximum oxidation rate (O_{max}), ability of plant-mediated transportation decided by species composition and plant density (T_{veg}), and optimum temperature for CH_4 production (T_{opt_pro}) with sensitivity index values higher than 0.2. T_{opt_pro} and r_me had the highest sensitivity index values throughout the growing season (sensitivity class >1.00, very high), suggesting the importance of temperature and soil substrate in methanogenesis to methane emission. Q_{10_pro}, O_{max}, and T_{veg} rank in the second class of sensitivity and the sensitivity index values varied across growing season. Q_{10}_pro had the lowest value of sensitivity index in July and October (around 0.2). O_{max}, and T_{veg} had the highest sensitivity index value in peak growing season (Aug, Sep and Oct, around 0.5), suggesting the importance of plant root transportation and oxidation on methane emission in response to environmental change.

There are strong interaction effects among r_me, Q_{10}_pro and T_{opt_pro} as these parameters are multiplied in the same equation for methane production. We settled a reasonable value of T_{opt_pro} to 20.0 based on published incubation results [*Wilson et al.*, 2016] and the values cited in other modeling papers (*Zhuang et al.*, 2004; *Zhu et al.*, 2014), so as to better constrain the other parameter values using data assimilation. Two out of 4 parameters put into data assimilation were constrained including r_me and Q_{10_pro} (Fig. 4). Histograms of parameter shows that the distribution of r_me is well constrained with a unimodal shape and the distribution of Q_{10_pro} is edge hitting with a marginal distribution upward (Fig. 4ab). T_{veg} and O_{max} has the largest variability

and wide, slightly-domed distributions (Fig. 4cd), which may have resulted from a limited number of observation data points and large variation in the CH_4 emission measurements.

3.2 Simulation, validation and forecast in ambient condition

Our simulated CH_4 flux well-captured the general seasonal changes in the CH_4 emission observed by the large collar chamber (Fig. 5). The mean annual methane efflux from 2011-2014 was 16.5 ± 2.0 g C m^{-2} yr^{-1}. We applied observational data from January 2015 - August 2016 for model forecasting validation (Fig. 5), with the parameters constrained in the data assimilation stage using the observational data from 2011-2014. During the forecasted period of 2015-2016, the seasonal changes of methane emission is well captured by the model (Fig. 5). To better show the seasonal variation, we picked the first year in the simulation (2011) and plotted daily variation of water table (simulated), surface soil temperature (measured), and methane emission (simulated) in panel a-c (Fig. 5). In general, the highest water table conditions occurred in late spring (May), and middle-to-late summer (July to August), while lower levels occurred in middle spring (April), early summer (June), and end of July. Before the month of July when the daily mean soil temperature was below 10 °C, methane emission was restricted by temperature. During the peak growing season the decrease of methane emission was mainly driven by low water level. When the water table was at or above the soil surface, CH_4 emission were more sensitive to variability in soil temperature. During the period from September 2016 - December 2024, the variation amplitudes of CH_4 emissions were relatively higher due to the statistically generated weather forcing data, while the general seasonal pattern remained the same with that from January 2011 - August 2016 (Fig. 5).

3.3 Responses of water table and CH_4 emission to warming and elevated CO_2

Our modeling results showed no significant changes of water table elevation in response to whole ecosystem warming treatment. By using constrained parameter values we were able to simulate CH_4 emission in the bog and found that warming significantly increased methane emission by 1.5, 2.1, 3.0, and 4.2 times under +2.25 ℃, +4.5 ℃, +6.75 ℃, and +9 ℃, respectively (Fig. 6a), while elevated CO_2 only had a small stimulating effect (*ca.* 10.4% - 28.6%) on methane emission (Fig. 6a). Both CH_4 production and oxidation increased by about 4 times above ambient level with 9 ˚C warming with enlarged uncertainties especially in the growing seasons (Fig. 6bc, Fig.8bc, 9bc). Plant-mediated transport is the major pathway of CH_4 emission which increased by *ca.* 4 times above the ambient level under 9 ˚C warming (Fig. 6d, 8adef, 9adef), however its relative contribution to methane emission decreased from 96% to 92% due to the increased ebullition (Fig. 7). At the same time, in ambient conditions the uncertainty of plant transported began to increase in early August (Fig. 8d), but the starting point moved up to late June under 9 ˚C warming (Fig. 9d). The absolute value of uncertainty was ten times the value without treatment. In ambient conditions, ebullition contributed 0.13% (0.02 g C m^{-2} yr^{-1}) of total emission, while under 9 ˚C warming the total amount of bubbles released into the atmosphere increased to 5.7% (4.0 g C m^{-2} yr^{-1}) of total emission (Fig. 7). The uncertainty in plant mediated transportation and ebullition both increased under warming (Fig. 6df), while the uncertainty in diffusion did not change much (Fig. 6e). The simulated results showed that diffusion contributed 3.4% (0.57 g C m^{-2} yr^{-1}) of total emission, and it decreased to 1.7% (1.17 g C m^{-2} yr^{-1}) of total emission under 9 ˚C warming (Fig. 7).

4. Discussion

4.1 Model performance in reducing uncertainties

Data-model fusion reduced the uncertainty of methane emission estimation by constraining the CH_4 and CO_2 ratio, and temperature sensitivity for CH_4 production. In our model, with 30 data points of daily methane emission from 2011 to 2014, 2 out of 4 parameters were well-constrained or marginally edge-hitting. *Gill et al.* [2017] estimated the mean value of CH_4 flux Q_{10} to be 5.63 (2.92-10.52 with 95% confidence interval) using a linearized Q_{10} function [*Humphreys et al.*, 2005] at the same study site during the 2015 growing season. Our constrained Q_{10} range was 2.34-6.33 with 95% confidence interval, which overlaps with but has a narrower range than the estimate by *Gill et al.* [2017].

Equifinality and identifiability are the symptoms of using only one data stream to constrain multiple parameters in a model [*Wang et al.*, 2001; *Braswell et al.*, 2005; *Luo et al.*, 2009; *Keenan et al.*, 2011]. *Oikawa et al.* [2016] used one year of half hourly eddy covariance CH_4 emission data and constrained 3 parameters in the CH_4 module of PEPRMT-DAMM model. Although the posterior ranges of 2 out of 4 of key parameters in TECO_SPRUCE_ME have been constrained and thus the uncertainty has been reduced, there is still some uncertainty due to the unconstrained parameter O_{max} and lack of observation data available to constrain the other 3 parameters to a smaller range. More parameters could be constrained with more measurement data available, such as more data points in an extended length of time, as well as CH_4 concentration and CH_4 oxidation in different soil layers.

Our simulated CH_4 flux captured the general seasonal changes in CH_4 emissions observed by the large collar chamber (Fig. 5). Seasonal variations in wetland CH_4 fluxes are mostly determined by temporal changes in peatland water volume and soil temperature [*Walter et al., 2001; Gedney et*

541 *al., 2004*]. We found that soil temperature was the restricting factor when below 10 °C, while
542 during the peak growing season the decrease of CH_4 emission was mainly determined by the lower
543 water table (Fig. 5). CH_4 emission was more sensitive to variability in soil temperature during the
544 wet time when the water table was at or above the soil surface.
545 For the purpose of reducing simulation uncertainties by using data assimilation to constrain the
546 key parameters value, we did not fully incorporate all the processes and scalers described in other
547 studies, such as the effect of competition between processes [*Riley et al.*, 2011], pH and redox
548 potential [*Cao et al.*, 1998; *Segers and Kengen*, 1998; *Zhu et al.*, 2014]. There are always trade-
549 offs between the desire to include all the mechanisms assumed to be important and 1) reducing
550 those uncertainties from assumed model structure; 2) lack of prior knowledge of non-key
551 parameter values; and 3) the computational cost when applying data assimilation.

552 **4.2 Warming and eCO_2 effects on CH_4 emission**

553 By using constrained parameter values we were able to simulate CH_4 emission in the bog wetland
554 and found an exponential increase under warming (Fig. 6a). *Wilson et al*. [2016] fitted seasonal
555 flux measurements against the average temperature from 1m to 2m below the hollow surface and
556 also found an exponential increase in CH_4 emission using chamber flux measurements, also as part
557 of SPRUCE. Methane emissions were most responsive to warming during the peak growing
558 season, which could explain greater uncertainty in growing season in response to warming
559 simulated by the model (Fig. 8a, 9a). We found elevated CO_2 had a small stimulating effect (*ca.*
560 10.4% - 28.6%) on methane emission (Fig. 6a), due to increased substrate supply for
561 methanogenesis. Because elevated CO_2 has stimulating effects on soil respiration in TECO model
562 through increased photosynthesis and thus increased substrate supply for mineralization [*Shi et al.*,
563 2015b].

We compared our results with other modelling and experimental work. The Wetland and Wetland CH_4 Inter Comparison of Models Project (WETCHIMP) simulated the change in global methane emission in response to temperature increase (+3.7 °C) and elevated CO_2 (step increase from ~300 to 857 ppm) using ten global models [*Melton et al.* 2013]. A ~160% increase in global CH_4 flux was found in ORCHIDEE model with the largest sensitivity to increased CO_2, other models results showed an increase of global CH_4 emission from 73.2% ±49.1% to 55.4%±25.5%. Our results showed that elevated CO_2 treatments stimulated methane emission by 10.4% - 23.6% per unit at site level. The difference may be attributable to their expectation of an ~13% increase of global wetland areal extent under the elevated CO_2 scenarios. Furthermore, different wetland types, such as bogs and fens, may respond differently to CO_2 enrichment [*Boardman et al.*, 2011].

Our findings of increased methane emission with CO_2 enrichment are also consistent with experiments. Methane emissions in natural wetlands and mesocosms generally have increased with exposure to elevated atmospheric CO_2 [*Megonigal and Schlesinger*, 1997; *Saarnio and Silvola,* 1999; *Saarnio et al*., 2003]. In a meta-analysis study, *van Groenigen et al.* [2011] reported an increase of methane emission from natural wetlands of 13.2% per area for an atmospheric CO_2 concentration increase from 473-780 ppm. In an incubation study, *Kang et al.* [2001] found no significant differences in CH_4 emission regardless a significantly higher biomass in a fen peatland. Our results showed a much stronger response of methane emission (30%, 100%, 275%, and 400% under 2.25, 4.5, 6.75, 9°C warming) mainly due to no significant changes in water table elevation in response to the whole ecosystem warming treatment in this area, which was in agreement with observed water table depth during the deep peat warming period [*Wilson et al.,* 2016]. The same pattern of water elevation under warming was also projected by CLM model at the same study site [*Shi et al.*, 2015a]. *Zhu et al.* [2011] estimated CH_4 emission in Northern Eurasia with the TEM

587 model for the period 1971–2100 (annual mean soil temperature gradually increased by ~6°C,
588 annual precipitation gradually increased by 30%). They found the water table dropped due to the
589 increased soil temperature, which diminished water table rising after additional rainfall. Using
590 various datasets on wetland extent, regional methane emission increased by 6-51%. Results from
591 WETCHIMP showed a slight, non-significant decline in global methane emission with warming
592 (+3.7 °C), due to a moderate decline in wetland area [*Melton et al*. 2013]. IAP is the only model
593 showing a large increase in CH_4 emissions, because it does not simulate increased evaporation
594 under warmer surface air temperature or an effect decreasing wetland area with increased
595 evaporation. Wetlands from different regions may also have differential responses to elevated
596 temperature. In warm regions, methane production may decreas if elevated temperature causes
597 down-regulation of photosynthesis and henceforth production of substrate for methane production
598 [*Melton et al*. 2013]. *Bohn et al.* [2007] used the VBM model and simulated methane emission in
599 western Siberia. They found increased methane production with higher temperature alone (0-5°C),
600 but overall shrinking of wetland area resulted in a net reduction in methane emissions.
601 Our simulation results showed that the total CH_4 production increased by 4 times under 9 ˚C
602 warming, while the heterotrophic respiration has only increased by *ca.* 25% in comparison to
603 ambient temperatures. That large contrast between methane production and respiration implies a
604 higher temperature dependence of methanogenesis than respiration. A similar result was also found
605 at the same site in an incubation study [*Wilson et al.*, 2016], where they found a positive correlation
606 between CH_4: CO_2 emission ratio and increased temperature. Consistently higher temperature
607 dependence in methanogenesis was also found across the ecosystem (field flux measurement),
608 community (CH_4 incubation), and species levels (pure culture) [*Yvon-Durocher et al.*, 2014].

609 We did not find differential responses of CH_4 emission in different layers, while the incubation
610 study by Wilson et al. [2016] showed that the increased CH_4 emission was largely driven by
611 surface peat (25cm) warming by measuring CH_4 production in different layers (25cm, 75cm,
612 100cm, 150cm and 200cm). The Q_{10} for CH_4 production (Q_{10}_pro) may vary in different soil layers
613 and this parameter value is important when estimating CH_4 emission under warming. Different
614 Q_{10} values for surface and catotelm soil may be needed in methane models. One possible solution
615 is to add o-alkyl carbon (C) content as a function of basal Q_{10} into the equation, because the lack
616 of reactivity from deep peat to warming was speculated to result from low o-alkyl C [*Leifeld et al.*,
617 2012; *Tfaily et al.*, 2014; *Wilson et al.*, 2016].
618 In order to eliminate the interaction effect between r_me, Q_{10}_pro and Topt_pro when constraining
619 their values, we set one of the key parameter Topt_pro (reference temperature for methanogenesis)
620 to 20 ˚C in this ecosystem. A wide range of Topt_pro values (-5.5 - 25 ˚C) have been used in
621 methane models for various ecosystems. Even in one single ecosystem type, for example, the
622 boreal forest, the value used in different models varies from 10 ˚C [*Zhuang et al.*, 2004] to 25 ˚C
623 [*Zhu et al.*, 2014]. As Topt_pro is an extremely sensitive parameter in TECO_SPRUCE_ME
624 model, we carefully estimated the value according to the temperature response of CH_4 production
625 from surface peat samples incubated within 1 ˚C of *in situ* temperatures from the same study site
626 [*Wilson et al.*, 2016]. In biogeochemical models all the reference temperatures for foliar respiration
627 [*Wythers et al.*, 2005], soil respiration [*Luo et al.*, 2001], and root respiration [*Atkin et al.*, 2000]
628 were set to constant values, even when the acclimation effect on Q_{10} and specific reaction rate at
629 a reference temperature were considered. This method was chosen partially because the reference
630 temperature is an intrinsic biological term which is stable under a certain combination of
631 organisms, for example, the structure of the microbial community, and the concentration and

quality of soil organic matter. On the other hand, the potential change in reference temperature due the change in depth and substrate supply could be reflected by the change in Q_{10}.

4.3 Differential responses of CH_4 emission pathways to warming and eCO_2

Removal of the vascular plants (*Eriophorum vaginatum*) in a Swedish boreal peatland decreased the seasonal CH_4 flux by 55%-85% [*Waddington et al.* 1996]. Wania *et al.* [2010] estimated the contribution of plant-mediated transport to be 67.8%-84.5% across different sites using the LPJ-WHyMe model. In Arctic tundra, plant-mediated transport represented 92%-98% of the net emission measured by static chamber (clipping 100%, 50%, 0% of the phytomass quantity within the sample chamber [*Morrissey and Livingston,* 1992]). Plant-mediated transport was 92-96.5% of total emission at our study site. The contribution of plant mediated CH_4 efflux to total emission may be underestimated in some biogeochemical models where trees, forbs and shrubs were not included either because of the low NPP contribution or assumptions about the capacity of these various plant types to mediate gas transport [*Wania et al.* 2010; *Zhuang et al.* 2004]. Lignified or suberized plants, such as trees, are considered incapable of transporting CH_4. However, in the past 10 years some studies have detected considerable CH_4 efflux from stems [*Terazawa et al.*, 2007; *Carmichael et al.*, 2014; *Pitz and Megonigal*, 2017]. Trees in boreal forests have been found to emit methane from both stems and shoots [Machacova *et al.*, 2016]. Tree-mediated CH_4 emissions contribute up to 27% of seasonal ecosystem CH4 flux in a temperate forested wetland [Pangala *et al.*, 2015]. In the TECO model, roots were not separated into tree, shrub, and grass, but we used a scaler T_{veg}, a parameter that was determined by type and plant density. This parameter represents the ability of plant to transport CH_4 at the community level. Plant-mediated transport of CH_4 from deep soil layers may have been over estimated as the trees and shrubs may transport less CH_4 than grasses and sedges. More data on the relative effects of different plant functional types on CH_4

transport are needed. For the long term projections, vegetation change should be considered as CH_4 emission is sensitive to T_{veg}. The constant value used for T_{veg} in global methane emission models [*Zhang et al.*, 2002; *Zhuang et al.*, 2004; *Riley et al.*, 2011; *Zhu et al.*, 2014] may bias for CH_4 emission estimates.

Diffusion accounts for ~5% on average in south Florida wetlands [*Barber et al.* 1988]. Ebullition accounts for 10% - 60% of the emission [*Chanton et al.* 1989; *Tokida et al.* 2007]. At the SPRUCE site, *Gill et al.* [2017] did chamber measurements but used 30 cm diameter collars to measure methane emissions at a smaller community level. Trees, shrubs and plants with well-developed aerenchyma tissues, such as *Eriophorum spissum*, were excluded at this measurement scale. They estimated 2015 growing season ebullition fluxes to be 1% of total CH_4 flux measurements averaged from different warming treatments by considering CH_4 fluxes > 2 standard deviations of the median as products of CH_4 ebullition. We estimated that diffusion and ebullition accounted for 3.4% and 0.1%, respectively. We found that CH_4 production rate drives the overall pattern of CH_4 emission (Fig7 ab). Due to a higher CH_4 concentration in soil layers, the relative contribution of ebullition increased from 0.13% at the control to 5.7% at the 9˚C warming, given the fact that any "excess" CH_4 is immediately released into the atmosphere when water table is above the soil surface. Although the absolute value of diffusion fluxes increased from 0.57 at the control to 1.17 g C m^{-2} yr^{-1} at the 9˚C warming, the relative contribution of diffusion decreased to 1.7% from 3.4%. Our model-simulation of ebullition matched the observational data, which implied that model-data fusion differentiates responses of plant-mediated transportation, diffusion, and ebullition to climate change. The uncertainty in plant-mediated transportation and ebullition increased under warming and contributed to the overall change of uncertainty in emission.

4.4 Future Studies

678 Existing methane models use a constant value of ecosystem-specific parameters such as Q_{10} for
679 CH_4 production (Q_{10}_pro) and potential ratio of anaerobically mineralized carbon released as CH_4
680 (r_me). Under long-term warming conditions, however, ecosystem acclimation to temperature
681 may result in a change in Q_{10} [*Wythers et al.*, 2005; *Gill et al.* 2017] and r_me. Through our data-
682 model fusion framework, the long-term change in parameter values may be detected by combining
683 the long term CH_4 emission measurement data and more data sets coming out such as CH_4
684 concentration in different layers and CH_4 oxidation rate.

5. Conclusions

We developed a methane module, which included processes of methane production, methane oxidation, plant mediated methane transportation, diffusion through different layers, and ebullition, together with water table dynamics. The methane module was integrated into the Terrestrial ECOsystem (TECO) model. After constraining the parameters with multiple years of methane emission data in a northern Minnesota peatland, we used the model to forecast CH_4 emission until 2024 under five warming and two elevated CO_2 treatments. We found 9 ˚C warming significantly increased methane emission by 4 times above ambient conditions, and elevated CO_2 stimulated methane emission by 10.4%-23.6%. The uncertainty in plant-mediated transportation and ebullition increased under warming and contributed to the overall change of uncertainty in CH_4 emission estimates. The model-data fusion approach used in this study enabled parameter estimation and uncertainty quantification for forecasting methane fluxes. As additional data for warming and elevated CO_2 treatments becomes available, the data-model fusion may help estimate parameter changes as ecosystems acclimate over time. The sensitivity of T_{opt_pro} and T_{veg} suggested that these could be key parameters to be measured in the field so as to reduce uncertainties in process-based models. Furthermore, the larger warming potential of CH_4 may result in a more positive feedback of global warming in terrestrial ecosystems.

Acknowledgements

We thank Russell Doughty for his English language editing of this manuscript. Xingjie Lu, Junyi Liang offered technical help on coding and debugging. This work was primarily founded by subcontract 4000144122 from Oak Ridge National Laboratory (ORNL) to the University of Oklahoma. Oak Ridge National Laboratory is managed by UT-Battelle, LLC, for the U.S. Department of Energy under contract DE-AC05-00OR22725. Research in Yiqi Luo's EcoLab was also financially supported by U.S. DOE DE-SC0008270, DE-SC00114085 and U.S. National Science Foundation (NSF) grant EF 1137293, OIA-1301789. All data sets from this study are available upon request. Relevant measurements were obtained from the SPRUCE webpage (http://mnspruce.ornl.gov/), the archival ftp site (ftp://sprucedata.ornl.gov), or from the USDA Forest Service. Data and source code of the TECO_SPRUCE_ME model are available at http://dx.doi.org/10.3334/CDIAC/spruce.046.

720 **References**

721 Atkin, O. K., E. J. Edwards, and B. R. Loveys (2000), Response of root respiration to changes in
722 temperature and its relevance to global warming, *New Phytol*., 147(1), 141–154, doi:
723 10.1046/j.1469-8137.2000.00683.x.

724 Barber, T. R., Burke, R. A., and Sackett, W. M. (1988). Diffusive flux of methane from warm
725 wetlands. *Global Biogeochemical Cycles*, 2(4), 411-425, doi: 10.1029/GB002i004p00411.

726 Bartlett, K. B., P. M. Crill, J. A. Bonassi, J. E. Richey, and R. C. Harriss (1990), Methane flux
727 from the Amazon River floodplain: Emissions during rising water, *J. Geophys. Res.*, *95*(D10),
728 16773, doi:10.1029/JD095iD10p16773.

729 Bender, M., and R. Conrad (1992), Kinetics of CH_4 oxidation in oxic soils exposed to ambient air
730 or high CH_4 mixing ratios, *FEMS Microbiol. Lett.*, *101*(4), 261–270, doi:10.1111/j.1574-
731 6968.1992.tb05783.x.

732 Bohn, T. J., Lettenmaier, D. P., Sathulur, K., Bowling, L. C., Podest, E., McDonald, K. C., and
733 Friborg, T. (2007). Methane emissions from western Siberian wetlands: heterogeneity and
734 sensitivity to climate change. *Environmental Research Letters*, 2(4), 045015, doi:10.1088/
735 1748-9326/2/4/045015.

736 Boardman, C. P., Gauci, V., Watson, J. S., Blake, S., and Beerling, D. J. (2011). Contrasting
737 wetland CH_4 emission responses to simulated glacial atmospheric CO_2 in temperate bogs and
738 fens. *New Phytologist*, 192(4), 898-911, doi: 10.1111/j.1469-8137.2011.03849.x.

739 Braswell, B. H., W. J. Sacks, E. Linder, and D. S. Schimel (2005), Estimating diurnal to annual
740 ecosystem parameters by synthesis of a carbon flux model with eddy covariance net
741 ecosystem exchange observations, *Glob. Chang. Biol.*, 11(2), 335–355, doi:10.1111/j.1365-
742 2486.2005.00897.x.

743 Bridgham, S. D., J. P. Megonigal, J. K. Keller, N. B. Bliss, and C. Trettin (2006), The carbon
744 balance of North American wetlands, *Wetlands*, 26(4), 889–916, doi: 10.1672/0277-
745 5212(2006)26[889:TCBONA]2.0.CO;2
746 Bridgham, S. D., H. Cadillo-Quiroz, J. K. Keller, and Q. Zhuang (2013), Methane emissions from
747 wetlands: biogeochemical, microbial, and modeling perspectives from local to global scales,
748 *Glob. Chang. Biol.*, *19*(5), 1325–1346, doi:10.1111/gcb.12131.
749 Bubier, J. L., T. R. Moore, L. Bellisario, N. T. Comer, and P. M. Crill (1995), Ecological controls
750 on methane emissions from a Northern Peatland Complex in the zone of discontinuous
751 permafrost, Manitoba, Canada, *Global Biogeochem. Cycles*, *9*(4), 455–470, doi:10.1029/
752 95GB02379.
753 Cao, M., J. B. Dent, and O. W. Heal (1995), Modeling methane emissions from rice paddies,
754 *Global Biogeochem. Cycles*, *9*(2), 183–195, doi:10.1029/94GB03231.
755 Cao, M., S. Marshall, and K. Gregson (1996), Global carbon exchange and methane emissions
756 from natural wetlands: Application of a process-based model, *J. Geophys. Res. Atmos.*,
757 101(D9), 14399–14414, doi:10.1029/96JD00219.
758 Cao, M., K. Gregson, and S. Marshall (1998), Global methane emission from wetlands and its
759 sensitivity to climate change, *Atmos. Environ.*, *32*(19), 3293–3299, doi: http://dx.doi.org/
760 10.1016/S1352-2310(98)00105-8.
761 Carmichael, M. J., E. S. Bernhardt, S. L. Bräuer, and W. K. Smith (2014), The role of vegetation
762 in methane flux to the atmosphere: should vegetation be included as a distinct category in the
763 global methane budget?, *Biogeochemistry*, *119*(1), 1–24, doi:10.1007/s10533-014-9974-1.
764 Chanton, J. P., and J. W. H. Dacey (1991), Effects of vegetation on methane flux, reservoirs, and
765 carbon isotopic composition, *Trace gas Emiss. by plants*, 65–92.

766 Chanton, J. P., Martens, C. S., and Kelley, C. A. (1989). Gas transport from methane-saturated,
767 tidal freshwater and wetland sediments. *Limnology and Oceanography*, 34(5), 807-819, doi:
768 10.4319/lo.1989.34.5.0807
769 Conrad, R. (1999), Contribution of hydrogen to methane production and control of hydrogen
770 concentrations in methanogenic soils and sediments, *FEMS Microbiol. Ecol.*, *28*(3), 193–202.
771 doi: 10.1111/j.1574-6941.1999.tb00575.x
772 Finzi A.C., Giasson M-A, Gill A.L. 2016. SPRUCE Autochamber CO_2 and CH_4 Flux Data for
773 SPRUCE Experimental Plots. Carbon Dioxide Information Analysis Center, Oak Ridge
774 National Laboratory, US Department of Energy, Oak Ridge, Tennessee, USA.
775 doi.org/10.3334/CDIAC/SPRUCE.016
776 Forster, P., Ramaswamy, V., Artaxo, P., Berntsen, T., Betts, R., Fahey, D.W., Haywood, J., Lean,
777 J., Lowe, D.C., Myhre, G., Nganga, J., Prinn, R., Raga, G., Schulz, M., & Van Dorland, R.
778 Miller, H.L. (Ed.). (2007). Changes in Atmospheric Constituents and in Radiative Forcing
779 Chapter 2. United Kingdom: Cambridge University Press.
780 Fiedler, S., and M. Sommer (2000), Methane emissions, groundwater levels and redox potentials
781 of common wetland soils in a temperate-humid climate, *Global Biogeochemical Cycles*,
782 14(4), 1081-1093, doi:10.1029/1999GB001255.
783 Frolking, S., and P. Crill (1994), Climate controls on temporal variability of methane flux from a
784 poor fen in southeastern New Hampshire: Measurement and modeling, *Global Biogeochem.*
785 *Cycles*, *8*(4), 385–397, doi:10.1029/94GB01839.
786 Frolking, S., N. Roulet, and J. Fuglestvedt (2006), How northern peatlands influence the Earth's
787 radiative budget: Sustained methane emission versus sustained carbon sequestration, *J.*
788 *Geophys. Res. Biogeosciences*, 111(G1), 385–397, doi:10.1029/2005JG000091.

789 Gedney, N., P. M. Cox, and C. Huntingford (2004), Climate feedback from wetland methane
790 emissions, Geophys. Res. Lett., 31(20). doi:10.1029/2004GL020919.
791 Gelman, A., and D. B. Rubin (1992), Inference from Iterative Simulation Using Multiple
792 Sequences, *Stat. Sci.*, *7*(4), 457–472.
793 Gerard, G., and J. Chanton (1993), Quantification of methane oxidation in the rhizosphere of
794 emergent aquatic macrophytes: defining upper limits, *Biogeochemistry*, *23*(2), 79–97,
795 doi:10.1007/BF00000444.
796 Gill, A. L., Giasson, M. A., Yu, R., and Finzi, A. C. (2017). Deep peat warming increases surface
797 methane and carbon dioxide emissions in a black spruce dominated ombrotrophic bog. *Global*
798 *Change Biology*, 00(1)-14, doi: 10.1111/gcb.13806
799 Granberg, G., H. Grip, M. O. Löfvenius, I. Sundh, B. H. Svensson, and M. Nilsson (1999), A
800 simple model for simulation of water content, soil frost, and soil temperatures in boreal mixed
801 mires, *Water Resour. Res.*, *35*(12), 3771–3782, doi:10.1029/1999WR900216.
802 Granberg, G., I. Sundh, B. H. Svensson, and M. Nilsson (2001), Effects of Temperature, and
803 Nitrogen and Sulfur Deposition, on Methane Emission from a Boreal Mire, *Ecology*, *82*(7),
804 1982–1998, doi:10.2307/2680063.
805 Griffiths, N. A., and Sebestyen, S. D. (2016). Dynamic vertical profiles of peat porewater
806 chemistry in a northern peatland. *Wetlands*, 36(6), 1119-1130. doi:10.1007/s13157-016-
807 0829-5.
808 Hanson, P. J. et al. (2016a), Attaining Whole-Ecosystem Warming Using Air and Deep Soil
809 Heating Methods with an Elevated CO_2 Atmosphere, *Biogeosciences Discuss.*, 1–48,
810 doi:10.5194/bg-2016-449.
811 Hanson, P. J., A. L. Gill, X. Xu, J. R. Phillips, D. J. Weston, R. K. Kolka, J. S. Riggs, and L. A.

Hook (2016b), Intermediate-scale community-level flux of CO_2 and CH_4 in a Minnesota peatland: putting the SPRUCE project in a global context, *Biogeochemistry*, *129*(3), 255–272, doi:10.1007/s10533-016-0230-8.

Hanson, P.J., J.R. Phillips, J.S. Riggs, and W.R. Nettles. 2017. SPRUCE Large-Collar In Situ CO_2 and CH_4 Flux Data for the SPRUCE Experimental Plots: Whole-Ecosystem-Warming. Carbon Dioxide Information Analysis Center, Oak Ridge National Laboratory, U.S. Department of Energy, Oak Ridge, Tennessee, U.S.A. http://dx.doi.org /10.3334/CDIAC/ spruce.034

Hayward, P. M., and R. S. Clymo (1982), Profiles of Water Content and Pore Size in Sphagnum and Peat, and their Relation to Peat Bog Ecology, *Proc. R. Soc. London B Biol. Sci.*, *215*(1200), 299–325, doi:10.1098/rspb.1982.0044.

Huang, Y., Jiang, J., Ma, S., Ricciuto, D., Hanson, P. J., and Luo, Y. (2017). Soil thermal dynamics, snow cover and frozen depth under five temperature treatments in an ombrotrophic bog: Constrained forecast with data assimilation. *Journal of Geophysical Research: Biogeosciences*, doi: 10.1002/2016JG003725

Humphreys, E. R., T. Andrew Black, K. Morgenstern, Z. Li, and Z. Nesic (2005), Net ecosystem production of a Douglas-fir stand for 3 years following clearcut harvesting, *Glob. Chang. Biol.*, *11*(3), 450–464, doi:10.1111/j.1365-2486.2005.00914.x.

Iversen CM, Childs J, Norby RJ et al. (2017) SPRUCE S1 Bog Fine-root Production and Standing Crop Assessed With Minirhizotrons in the Southern and Northern Ends of the S1 Bog. Carbon Dioxide Information Analysis Center, Oak Ridge National Laboratory, U.S. Department of Energy, Oak Ridge, Tennessee, USA, http://dx.doi.org/10.3334/CDIAC/spruce.019.

Jiang, J., S. Ma, Y. Huang, D. Ricciuto, P. J. Hanson, and Y. Luo (2017), Forecasting responses

of a northern peatland carbon cycle to elevated CO_2 and a gradient of experimental warming (in revision)

Joabsson, A., T. R. Christensen, and B. Wallén (1999), Vascular plant controls on methane emissions from northern peatforming wetlands, *Tree*, *14*. doi: http://dx.doi.org/10.1016/S0169-5347 (99)01649-3.

Kang, H., Freeman, C., and Ashendon, T. W. (2001). Effects of elevated CO_2 on fen peat biogeochemistry. *Science of the Total Environment*, 279(1), 45-50, doi: https://doi.org/10.1016/S0048-9697(01)00724-0.

Keenan, T. F., M. S. Carbone, M. Reichstein, and A. D. Richardson (2011), The model--data fusion pitfall: assuming certainty in an uncertain world, *Oecologia*, *167*(3), 587, doi:10.1007/s00442-011-2106-x.

Keenan, T. F., E. A. Davidson, J. W. Munger, and A. D. Richardson (2012), Rate my data: quantifying the value of ecological data for the development of models of the terrestrial carbon cycle, *Ecol. Appl.*, *23*(1), 273–286, doi:10.1890/12-0747.1.

Kettunen, A., V. Kaitala, A. Lehtinen, A. Lohila, J. Alm, J. Silvola, and P. J. Martikainen (1999), Methane production and oxidation potentials in relation to water table fluctuations in two boreal mires, *Soil Biol. Biochem.*, *31*(12), 1741–1749, doi:10.1016/S0038-0717(99)00093-0.

Leifeld, J., M. Steffens, and A. Galego-Sala (2012), Sensitivity of peatland carbon loss to organic matter quality, *Geophys. Res. Lett.*, *39*(14), n/a-n/a, doi:10.1029/2012GL051856.

Le Mer, J., & Roger, P. (2001). Production, oxidation, emission and consumption of methane by soils: a review. *European Journal of Soil Biology*, 37(1), 25-50, doi: https://doi.org/10.1016/S1164-5563(01)01067-6.

Lenhart, T., K. Eckhardt, N. Fohrer, and H.-G. Frede (2002), Comparison of two different

approaches of sensitivity analysis, *Phys. Chem. Earth, Parts A/B/C*, *27*(9–10), 645–654, doi:http://dx.doi.org/10.1016/S1474-7065(02)00049-9.

Luo, Y., and J. F. Reynolds (1999), Validity of extrapolating field CO_2 experiments to predict carbon sequestration in natural ecosystems, *Ecology*, *80*(5), 1568–1583. doi: 10.1890/0012-9658(1999)080[1568:VOEFCE]2.0.CO;2

Luo, Y., S. Wan, D. Hui, and L. L. Wallace (2001), Acclimatization of soil respiration to warming in a tall grass prairie, *Nature*, *413*(6856), 622–625. doi:10.1038/35098065

Luo, Y., E. Weng, X. Wu, C. Gao, X. Zhou, and L. Zhang (2009), Parameter identifiability, constraint, and equifinality in data assimilation with ecosystem models, *Ecol. Appl.*, *19*(3), 571–574, doi:10.1890/08-0561.1.

Luo, Y., A. Ahlström, S. D. Allison, N. H. Batjes, V. Brovkin, N. Carvalhais, A. Chappell, P. Ciais, E. A. Davidson, and A. Finzi (2015), Towards More Realistic Projections of Soil Carbon Dynamics by Earth System Models, Global Biogeochem. Cycles. doi: 10.1002/2015GB005239

Machacova, K., Bäck, J., Vanhatalo, A., Halmeenmäki, E., Kolari, P., Mammarella, I., Pumpanen, J., Acosta, M., Urban, O. and Pihlatie, M., 2016. Pinus sylvestris as a missing source of nitrous oxide and methane in boreal forest. *Scientific reports*, 6. doi:10.1038/srep23410

Megonigal, J. P., and Schlesinger, W. H. (1997). Enhanced CH_4 emission from a wetland soil exposed to elevated CO_2. *Biogeochemistry*, 37(1), 77-88, doi: https://doi.org/10.1023/A:1005738102545.

Melton, J. R., Wania, R., Hodson, E. L., Poulter, B., Ringeval, B., Spahni, R., Bohn T, Avis C.A., Beerling D.J., Chen G., and Eliseev, A. V. (2013). Present state of global wetland extent and wetland methane modelling: conclusions from a model intercomparison project

881 (WETCHIMP). *Biogeosciences*, 10, 753-788, doi: https://doi.org/10.5194/bg-10-753-2013.
882 Meng, L., P. G. M. Hess, N. M. Mahowald, J. B. Yavitt, W. J. Riley, Z. M. Subin, D. M. Lawrence,
883 S. C. Swenson, J. Jauhiainen, and D. R. Fuka (2012), Sensitivity of wetland methane
884 emissions to model assumptions: application and model testing against site observations,
885 *Biogeosciences*, *9*(7), 2793–2819, doi:10.5194/bg-9-2793-2012.
886 Morrissey, L. A., and G. P. Livingston (1992), Methane emissions from Alaska Arctic tundra: An
887 assessment of local spatial variability, *Journal of Geophysical Research: Atmospheres*,
888 97(D15), 16661-16670, doi:10.1029/92JD00063.
889 Neubauer, S. C., and J. P. Megonigal (2015), Moving Beyond Global Warming Potentials to
890 Quantify the Climatic Role of Ecosystems, *Ecosystems*, *18*(6), 1000–1013, doi:10.1007/
891 s10021-015-9879-4.
892 Oikawa, P. Y., G. D. Jenerette, S. H. Knox, C. Sturtevant, J. Verfaillie, I. Dronova, C. M.
893 Poindexter, E. Eichelmann, and D. D. Baldocchi (2016), Evaluation of a hierarchy of models
894 reveals importance of substrate limitation for predicting carbon dioxide and methane
895 exchange in restored wetlands, *J. Geophys. Res. Biogeosciences*,
896 doi:10.1002/2016JG003438.
897 Pangala, S. R., Hornibrook, E. R., Gowing, D. J., & Gauci, V. (2015). The contribution of trees to
898 ecosystem methane emissions in a temperate forested wetland. *Global change biology*, 21(7),
899 2642-2654. doi: 10.1111/gcb.12891
900 Parsekian, A. D., Slater, L., Ntarlagiannis, D., Nolan, J., Sebesteyen, S. D., Kolka, R. K., &
901 Hanson, P. J. (2012). Uncertainty in peat volume and soil carbon estimated using ground-
902 penetrating radar and probing. *Soil Science Society of America Journal*, 76(5), 1911-1918,
903 doi:10.2136/sssaj2012.0040

904 Pitz, S., and J. P. Megonigal (2017), Temperate forest methane sink diminished by tree emissions,
905 *New Phytol.*, n/a--n/a, doi:10.1111/nph.14559.
906 Richardson, A. D. et al. (2010), Estimating parameters of a forest ecosystem C model with
907 measurements of stocks and fluxes as joint constraints, *Oecologia*, *164*(1), 25–40,
908 doi:10.1007/s00442-010-1628-y.
909 Riley, W. J., Z. M. Subin, D. M. Lawrence, S. C. Swenson, M. S. Torn, L. Meng, N. M. Mahowald,
910 and P. Hess (2011), Barriers to predicting changes in global terrestrial methane fluxes:
911 analyses using CLM4Me, a methane biogeochemistry model integrated in CESM,
912 *Biogeosciences*, *8*(7), 1925–1953, doi:10.5194/bg-8-1925-2011.
913 Roulier, S., and N. Jarvis (2003), Analysis of Inverse Procedures for Estimating Parameters
914 Controlling Macropore Flow and Solute Transport in the Dual-Permeability Model MACRO,
915 *Vadose Zo. J.*, *2*(3), 349–357, doi:10.2136/vzj2003.3490.
916 Saarnio, S., and Silvola, J. (1999). Effects of increased CO_2 and N on CH_4 efflux from a boreal
917 mire: a growth chamber experiment. *Oecologia*, 119(3), 349-356, doi: https://doi.org/
918 10.1007/s004420050795.
919 Saarnio, S., Järviö, S., Saarinen, T., Vasander, H., and Silvola, J. (2003). Minor changes in
920 vegetation and carbon gas balance in a boreal mire under a raised CO_2 or NH_4NO_3 supply.
921 *Ecosystems*, 6(1), 0046-0060, doi: https://doi.org/10.1007/s10021-002-0208-3.
922 Schipper, L. A., and K. R. Reddy (1996), Determination of Methane Oxidation in the Rhizosphere
923 of *Sagittaria lancifolia* Using Methyl Fluoride, *Soil Sci. Soc. Am. J.*, *60*(2), 611–616,
924 doi:10.2136/sssaj1996.03615995006000020039x.
925 Sebestyen, S. D., E. S. Verry, and K. N. Brooks (2011a), *Hydrological responses to forest cover*
926 *changes on uplands and peatlands, in: Peatland biogeochemistry and watershed hydrology*

927 *at the Marcell Experimental Forest*, Peatland biogeochemistry and watershed hydrology at
928 the Marcell Experimental Forest, CRC Press, New York.
929 Sebestyen, S. D., C. Dorrance, D. M. Olson, E. S. Verry, R. K. Kolka, A. E. Elling, and R.
930 Kyllander (2011b), Long-term monitoring sites and trends at the Marcell Experimental
931 Forest, *Peatl. Biogeochem. watershed Hydrol. Marcell Exp. For. CRC Press. Boca Raton,*
932 *FL*, 15–72.
933 Sebestyen S.D., Griffiths NA. 2016. SPRUCE Enclosure Corral and Sump System: Description,
934 Operation, and Calibration. Climate Change Science Institute, Oak Ridge National
935 Laboratory, U.S. Department of Energy, Oak Ridge, Tennessee, U.S.A. http://dx.doi.org/
936 10.3334/CDIAC/ spruce.030
937 Segers, R., and S. W. M. Kengen (1998), Methane production as a function of anaerobic carbon
938 mineralization: A process model, *Soil Biol. Biochem.*, *30*(8–9), 1107–1117, doi:
939 http://dx.doi.org/10.1016/S0038-0717(97)00198-3.
940 Shannon, R. D., and J. R. White (1994), A three-year study of controls on methane emissions from
941 two Michigan peatlands, *Biogeochemistry*, *27*(1), 35–60, doi:10.1007/BF00002570.
942 Shannon, R. D., J. R. White, J. E. Lawson, and B. S. Gilmour (1996), Methane Efflux from
943 Emergent Vegetation in Peatlands, *J. Ecol.*, *84*(2), 239–246. doi: 10.2307/2261359
944 Shea, K., M. R. Turetsky, and J. M. Waddington (2010), Quantifying diffusion, ebullition, and
945 plant-mediated transport of CH_4 in Alaskan peatlands undergoing permafrost thaw, *AGU*.
946 Shi, X., P. E. Thornton, D. M. Ricciuto, P. J. Hanson, J. Mao, S. D. Sebestyen, N. A. Griffiths, and
947 G. Bisht (2015a), Representing northern peatland microtopography and hydrology within the
948 Community Land Model, *Biogeosciences*, *12*(21), 6463–6477, doi:10.5194/bg-12-6463-
949 2015.

950 Shi, Z., Y. Yang, X. Zhou, E. Weng, A. C. Finzi, and Y. Luo (2015b), Inverse analysis of coupled
951 carbon-nitrogen cycles against multiple datasets at ambient and elevated CO_2, *J. Plant Ecol.*,
952 doi:10.1093/jpe/rtv059.
953 Shurpali, N. J., & Verma, S. B. (1998). Micrometeorological measurements of methane flux in a
954 Minnesota peatland during two growing seasons. *Biogeochemistry*, 40(1), 1-15, doi:
955 https://doi.org/10.1023/A:1005875307146.
956 Smith, M. J., D. W. Purves, M. C. Vanderwel, V. Lyutsarev, and S. Emmott (2013), The climate
957 dependence of the terrestrial carbon cycle, including parameter and structural uncertainties,
958 *Biogeosciences*, *10*(1), 583–606, doi:10.5194/bg-10-583-2013.
959 Spahni, R. et al. (2011), Constraining global methane emissions and uptake by ecosystems,
960 *Biogeosciences*, *8*(6), 1643–1665, doi:10.5194/bg-8-1643-2011.
961 Terazawa, K., S. Ishizuka, T. Sakata, K. Yamada, and M. Takahashi (2007), Methane emissions
962 from stems of Fraxinus mandshurica var. japonica trees in a floodplain forest, *Soil Biol.*
963 *Biochem.*, *39*(10), 2689–2692, doi:http://doi.org/10.1016/j.soilbio.2007.05.013.
964 Tfaily, M. M., W. T. Cooper, J. E. Kostka, P. R. Chanton, C. W. Schadt, P. J. Hanson, C. M.
965 Iversen, and J. P. Chanton (2014), Organic matter transformation in the peat column at
966 Marcell Experimental Forest: Humification and vertical stratification, *J. Geophys. Res.*
967 *Biogeosciences*, *119*(4), 661–675, doi:10.1002/2013JG002492.
968 Tokida, T., Miyazaki, T., Mizoguchi, M., Nagata, O., Takakai, F., Kagemoto, A., and Hatano, R.
969 (2007). Falling atmospheric pressure as a trigger for methane ebullition from peatland. *Global*
970 *Biogeochemical Cycles*, 21(2), doi: 10.1029/2006GB002790.
971 Turetsky, M. R., C. C. Treat, M. P. Waldrop, J. M. Waddington, J. W. Harden, and A. D. McGuire
972 (2008), Short-term response of methane fluxes and methanogen activity to water table and

973 soil warming manipulations in an Alaskan peatland, *J. Geophys. Res.*, *113*, G00A10,
974 doi:10.1029/2007JG000496.
975 Updegraff, K., S. D. Bridgham, J. Pastor, P. Weishampel, and C. Harth (2001), Response of CO_2
976 and CH_4 emissions from peatlands to warming and water table manipulation, *Ecol Appl*, *11*.
977 doi: 10.1890/1051-0761(2001)011[0311:ROCACE]2.0.CO;2
978 Van Groenigen, K. J., Osenberg, C. W., and Hungate, B. A. (2011). Increased soil emissions of
979 potent greenhouse gases under increased atmospheric CO_2. *Nature*, 475(7355), 214,
980 doi:10.1038/nature10176.
981 Verry, E.S. (1984), Microtopography and water table fluctuation in a Sphagnum mire. In:
982 Proceedings of the 7th International Peat Congress, Dublin, Ireland. The Irish National Peat
983 Committee / The International Peat Society, 11-31
984 Verville, J. H., S. E. Hobbie, F. S. Chapin, and D. U. Hooper (1998), Response of tundra CH_4 and
985 CO_2 flux to manupulation of temperature and vegetation, *Biogeochemistry*, *41*,
986 doi:10.1023/a:1005984701775.
987 Waddington, J. M., Roulet, N. T., & Swanson, R. V. (1996). Water table control of CH_4 emission
988 enhancement by vascular plants in boreal peatlands. *Journal of Geophysical Research:*
989 *Atmospheres*, 101(D17), 22775-22785. doi: 10.1029/96JD02014.
990 Walter, B. P., and M. Heimann (2000), A process-based, climate-sensitive model to derive
991 methane emissions from natural wetlands: Application to five wetland sites, sensitivity to
992 model parameters, and climate, *Global Biogeochem. Cycles*, *14*(3), 745–765,
993 doi:10.1029/1999GB001204.
994 Walter, B. P., M. Heimann, and E. Matthews (2001), Modeling modern methane emissions from
995 natural wetlands 1. Model description and results, J. Geophys. Res, 106(34), 134–189. doi:

996 10.1029/2001JD900165 doi: 10.1029/2001JD900165.
997 Wang, Y.-P., and R. Leuning (1998), A two-leaf model for canopy conductance, photosynthesis
998 and partitioning of available energy I:: Model description and comparison with a multi-
999 layered model, *Agric. For. Meteorol.*, *91*(1), 89–111. doi: https://doi.org/10.1016/S0168-
1000 1923(98)00061-6.
1001 Wang, Y.-P., R. Leuning, H. A. Cleugh, and P. A. Coppin (2001), Parameter estimation in surface
1002 exchange models using nonlinear inversion: how many parameters can we estimate and which
1003 measurements are most useful?, *Glob. Chang. Biol.*, *7*(5), 495–510, doi:10.1046/j.1365-
1004 2486.2001.00434.x.
1005 Wang, Y.-P., C. M. Trudinger, and I. G. Enting (2009), A review of applications of model–data
1006 fusion to studies of terrestrial carbon fluxes at different scales, *Agric. For. Meteorol.*, *149*(11),
1007 1829–1842, doi:http://dx.doi.org/10.1016/j.agrformet.2009.07.009.
1008 Wania, R., I. Ross, and I. C. Prentice (2009a), Integrating peatlands and permafrost into a dynamic
1009 global vegetation model: 1. Evaluation and sensitivity of physical land surface processes,
1010 *Global Biogeochem. Cycles*, *23*(3), n/a-n/a, doi:10.1029/2008GB003412.
1011 Wania, R., Ross, I., and Prentice, I. C. (2010), Implementation and evaluation of a new methane
1012 model within a dynamic global vegetation model: LPJ-WHyMe v1. 3.1. *Geoscientific Model*
1013 *Development*, 3(2), 565-584, doi: https://doi.org/10.5194/gmd-3-565-2010.
1014 Weng, E., and Y. Luo (2008), Soil hydrological properties regulate grassland ecosystem responses
1015 to multifactor global change: A modeling analysis, *J. Geophys. Res. Biogeosciences*,
1016 *113*(G3). doi: 10.1029/2007JG000539
1017 Whalen, S. C., and W. S. Reeburgh (1992), Interannual variations in tundra methane emission: A
1018 4-year time series at fixed sites, *Global Biogeochem. Cycles*, *6*(2), 139-159, doi:10.1029/

92GB00430.

Whalen, S. C. (2005). Biogeochemistry of methane exchange between natural wetlands and the atmosphere. *Environmental Engineering Science*, 22(1), 73-94, doi: https://doi.org/10.1089/ees. 2005.22.73

Whiting, G. J., and J. P. Chanton (1992), Plant-dependent CH_4 emission in a subarctic Canadian fen, *Global Biogeochem. Cycles*, *6*(3), 225–231, doi:10.1029/92GB00710.

Wilson, R. M. et al. (2016), Stability of peatland carbon to rising temperatures, *Nat. Commun.*, *7*, 13723, doi:10.1038/ncomms13723

Wythers, K. R., P. B. Reich, M. G. Tjoelker, and P. B. Bolstad (2005), Foliar respiration acclimation to temperature and temperature variable Q_{10} alter ecosystem carbon balance, *Glob. Chang. Biol.*, *11*(3), 435–449, doi:10.1111/j.1365-2486.2005.00922.x.

Xu, T., L. White, D. Hui, and Y. Luo (2006), Probabilistic inversion of a terrestrial ecosystem model: Analysis of uncertainty in parameter estimation and model prediction, *Global Biogeochem. Cycles*, *20*(2). doi: 10.1029/2005GB002468.

Yvon-Durocher, G., A. P. Allen, D. Bastviken, R. Conrad, C. Gudasz, A. St-Pierre, N. Thanh-Duc, and P. A. del Giorgio (2014), Methane fluxes show consistent temperature dependence across microbial to ecosystem scales, *Nature*, *507*(7493), 488–491, doi:10.1038/nature13164.

Zhang, Y., C. Li, C. C. Trettin, H. Li, and G. Sun (2002), An integrated model of soil, hydrology, and vegetation for carbon dynamics in wetland ecosystems, *Global Biogeochem. Cycles*, *16*(4), 9–17, doi:10.1029/2001GB001838.

Zhu, Q., J. Liu, C. Peng, H. Chen, X. Fang, H. Jiang, G. Yang, D. Zhu, W. Wang, and X. Zhou (2014), Modelling methane emissions from natural wetlands by development and application of the TRIPLEX-GHG model, *Geosci. Model Dev.*, *7*(3), 981–999, doi:10.5194/gmd-7-981-

2014.

Zhu, X., Zhuang, Q., Chen, M., Sirin, A., Melillo, J., Kicklighter, D., Sokolov A., and Song, L. (2011). Rising methane emissions in response to climate change in Northern Eurasia during the 21st century. *Environmental Research Letters*, 6(4), 045211, doi:10.1088/1748-9326/6/4/045211.

Zhuang, Q., J. M. Melillo, D. W. Kicklighter, R. G. Prinn, A. D. McGuire, P. A. Steudler, B. S. Felzer, and S. Hu (2004), Methane fluxes between terrestrial ecosystems and the atmosphere at northern high latitudes during the past century: A retrospective analysis with a process-based biogeochemistry model, *Global Biogeochem. Cycles*, *18*(3), n/a-n/a, doi:10.1029/2004GB002239.

1053 **Table 1**. Major parameters in CH_4 production, oxidation, diffusion, ebullition and plant mediated
1054 transportation. Parameters in bold indicate the ones used for initial sensitivity test. Parameters with
1055 a range indicate the model is sensitive to their values and are used for data assimilation.
1056

Process	Parameters	Values	Range	Unit	Description	References
CH_4 production	**r_me**	0.65	[0.0,0.7]	-	Potential ratio of anaerobically mineralized C released as CH_4	*Zhuang et al*. [2004], Segers [1998], *Zhu et al*. [2014]
	Q_{10}_pro	7.2	[0.0,10]	-	Q_{10} for CH_4 production	*Walter and Heimann* [2000]
	Topt_pro	20.0		℃	Optimum temperature for CH_4 production	*Wilson et al*. [2016]
CH_4 oxidation	**K_{CH4}**	5.0	-	μmol L^{-1}	Michaelis_Menten coefficients	*Walter and Heimann* [2000], *Zhang et al*. [2002],
	O_{max}	15.0	[3.0,45.0]	μmol L^{-1} h^{-1}	Maximum oxidation rate	*Zhuang et al*. [2004]
	Q_{10}_oxi	2.0	-	-	Q_{10} for CH_4 oxidation	*Walter and Heimann* [2000], *Meng et al*. [2012]
	Topt_oxi	10.0		℃	Optimum temperature for CH_4 production	*Zhuang et al.* [2004]
CH_4 diffusion	f_{tort}	0.66	-	-	Tortuosity coefficient	*Walter and Heimann* [2000]
	D_{air}	0.2	-	cm^2s^{-1}	Molecular diffusion coefficient of CH_4 in air	*Walter and Heimann* [2000]
	D_{water}	0.00002		cm^2s^{-1}	Molecular diffusion coefficient of CH_4 in water	*Walter and Heimann* [2000]
CH_4 ebullition	**$[CH_4]_{thre}$**	750	-	μmol L^{-1}	CH_4 concentration threshold above which ebullition occurs	*Walter and Heimann* [2000], *Zhu et al*. [2014]
Plant-mediated transportation	**T_{veg}**	0.7	[0.01,15.0]	-	factor of transport ability at plant community level	*Walter* [1998], *Zhuang et al.* [2004]

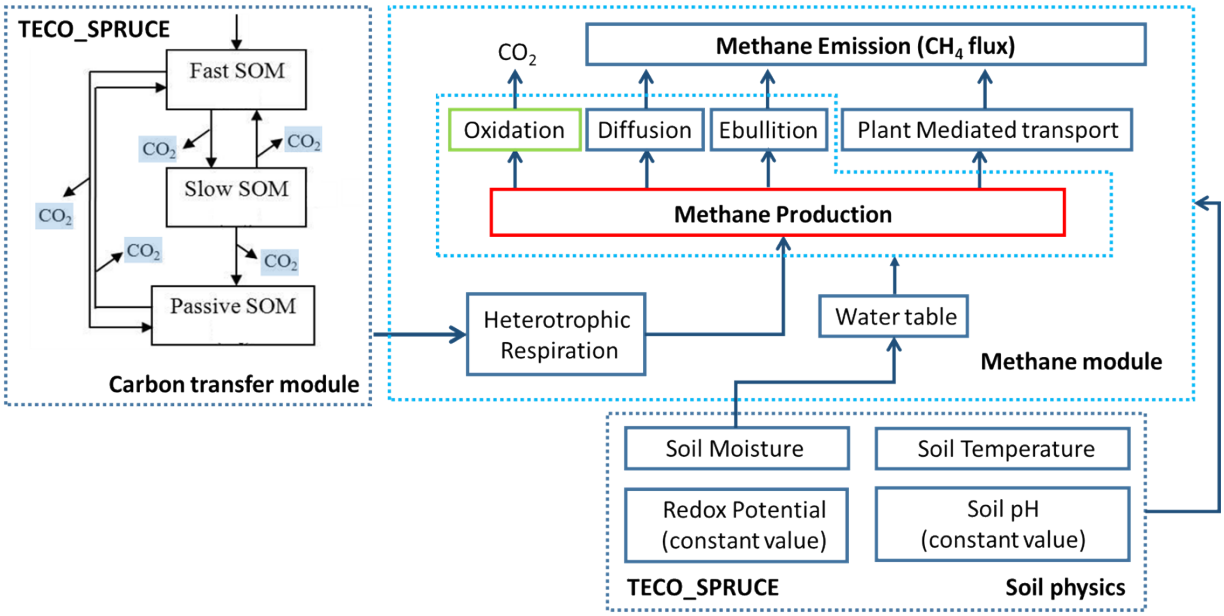

1058

1059 **Figure 1.** Conceptual structure and integration of water table and CH_4 emission modules into

1060 TECO_SPRUCE

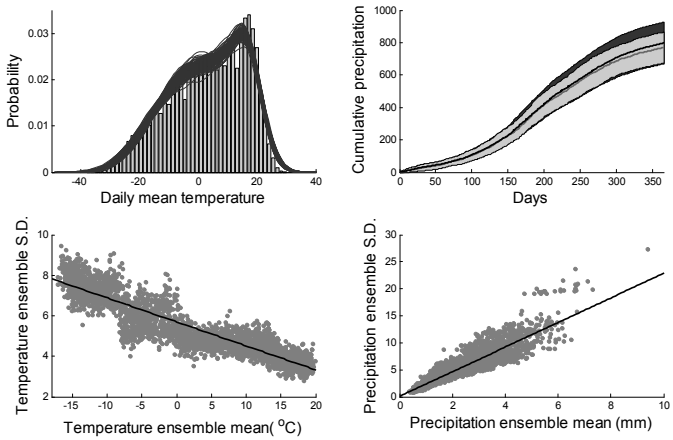

Figure 2. Historical climate from the USDA MEF site during 1961-2014, and stochastic weather generation for 2015-2024. (a) Probability density distribution of daily mean temperature (gray bar graph represents historical observation data, black curves represent ensemble of predicted future temperatures). (b) Cumulative precipitation within a year (curve and shaded areas represent mean and standard deviation, respectively; gray is historical observation data, and black is future predictions). (c) and (d) are standard deviations versus means for daily air temperature and precipitation, respectively. Credits from *Jiang Jiang et al.* [2017].

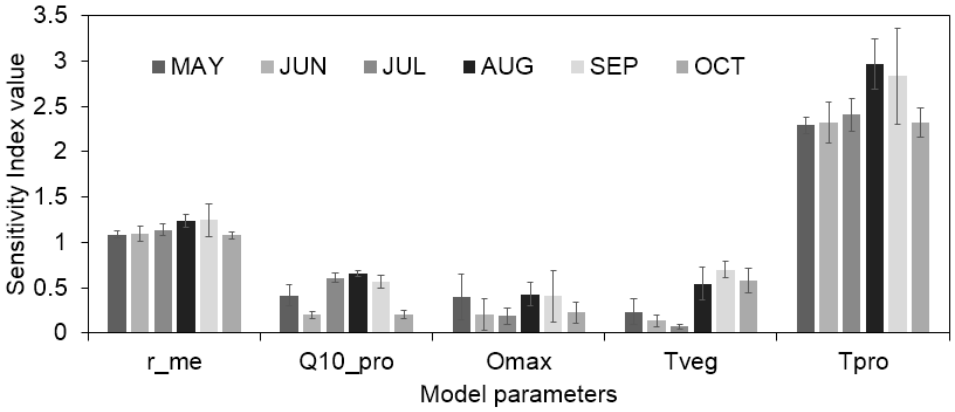

Figure 3. Sensitivity index for the most influential parameters for CH_4 fluxes during the growing season (4-year average of 2011-2014) in May, June, July, August, September and October. The error bar denotes standard deviation.

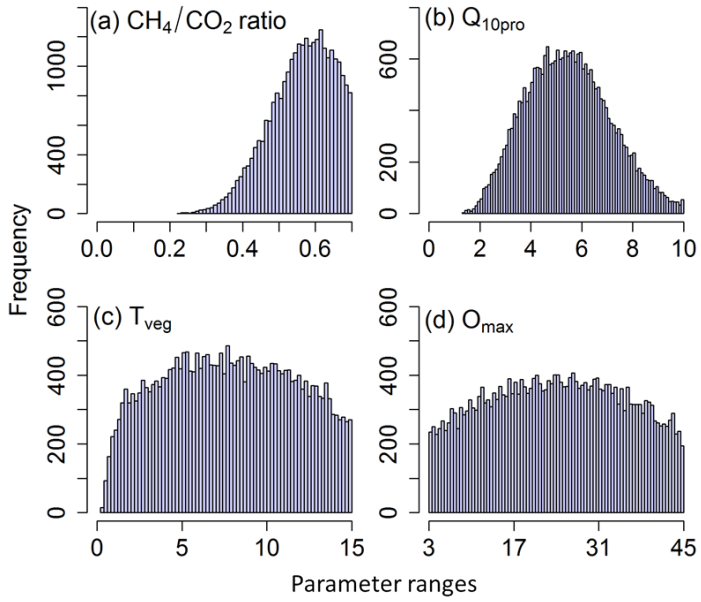

Figure 4. Posterior distributions of parameters of 50,000 samples from M-H simulation. (a), potential ratio of anaerobically mineralized carbon released as CH_4; (b), Q10 for CH_4 production; (c), maximum oxidation rate; (d) factor of transport ability at plant community level.

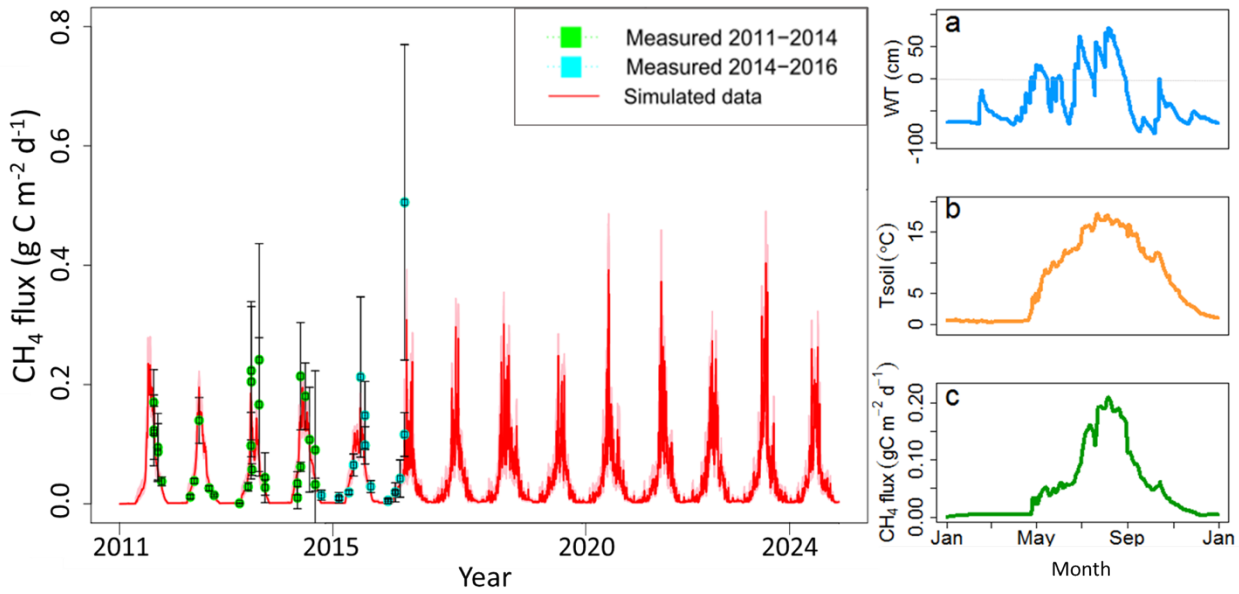

Figure. 5. Forecasting of CH_4 emission dynamics based on stochastically generated weather forcing data. Green dots refer to observations from 2011-2014 which were used for data assimilation. Blue dots indicate observations from 2015-2016 which were used for model validation, error bars indicate the standard deviation of each observation. Red line is simulated mean methane emission. The shading area corresponds to 1 standard deviation based on 500 randomly chosen model simulations with parameters drawn from the posterior distribution. Panel a-b are 2011 daily variation of water table, surface soil temperature, and methane emission.

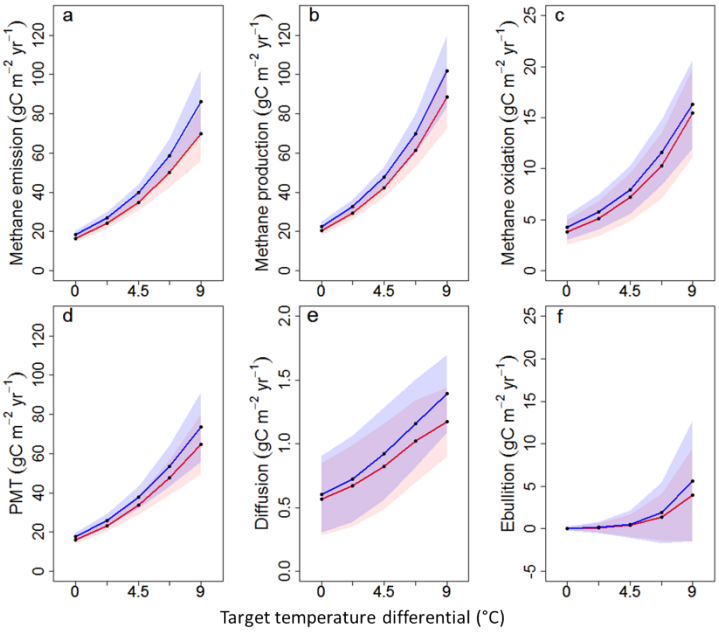

Figure 6. Responses of annual CH_4 emission to warming and elevated CO_2 (eCO_2). Red lines indicate CH_4 fluxes under warming treatments and 380 ppm CO_2, blue lines indicate CH_4 fluxes under warming treatments and 880 ppm CO_2. X-axes indicate the warming treatments of +0°C, +2.25°C, +4.5°C, +6.75°C and +9 °C above ambient level. Shading area correspond to mean ± one standard deviation based on 500 randomly chosen model simulations with parameters drawn from the posterior distribution.

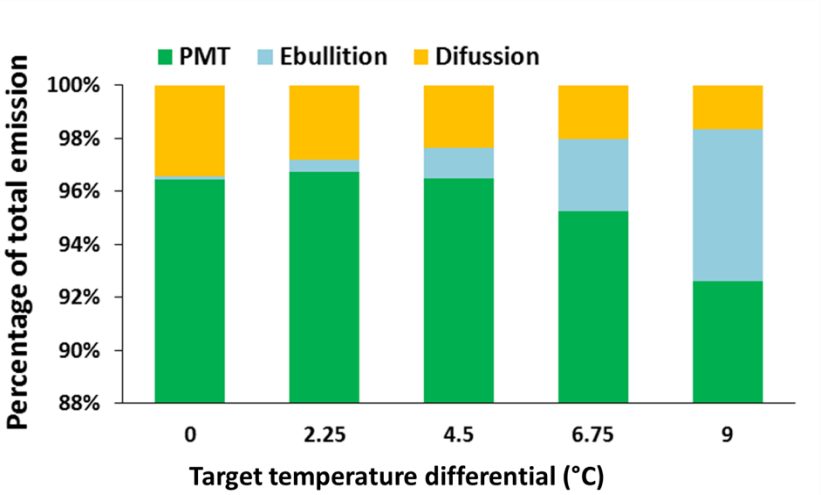

Figure 7. Simulated percentage of total emission in different pathways (plant-mediated transportation (PMT), ebullition, and diffusion) using the mean value from 100 accepted parameter sets.

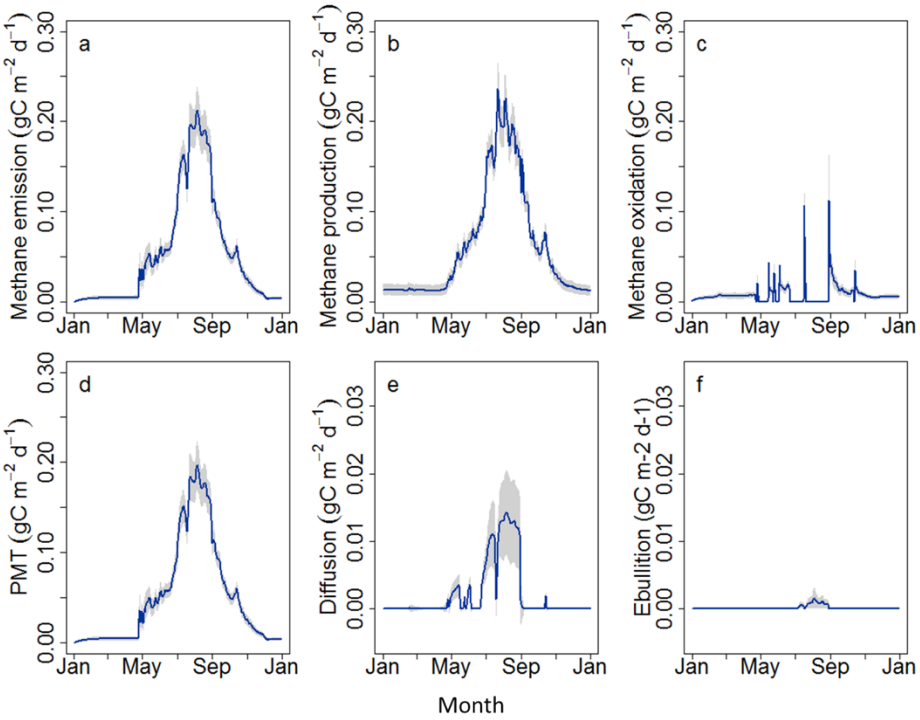

Figure 8. Simulated seasonal methane fluxes variation in 2011 under ambient condition. Blue lines indicate CH_4 fluxes under ambient temperature and 380 ppm CO_2. Shading areas correspond to mean ± one standard deviation based on 500 randomly chosen model simulations with parameters drawn from the posterior distribution.

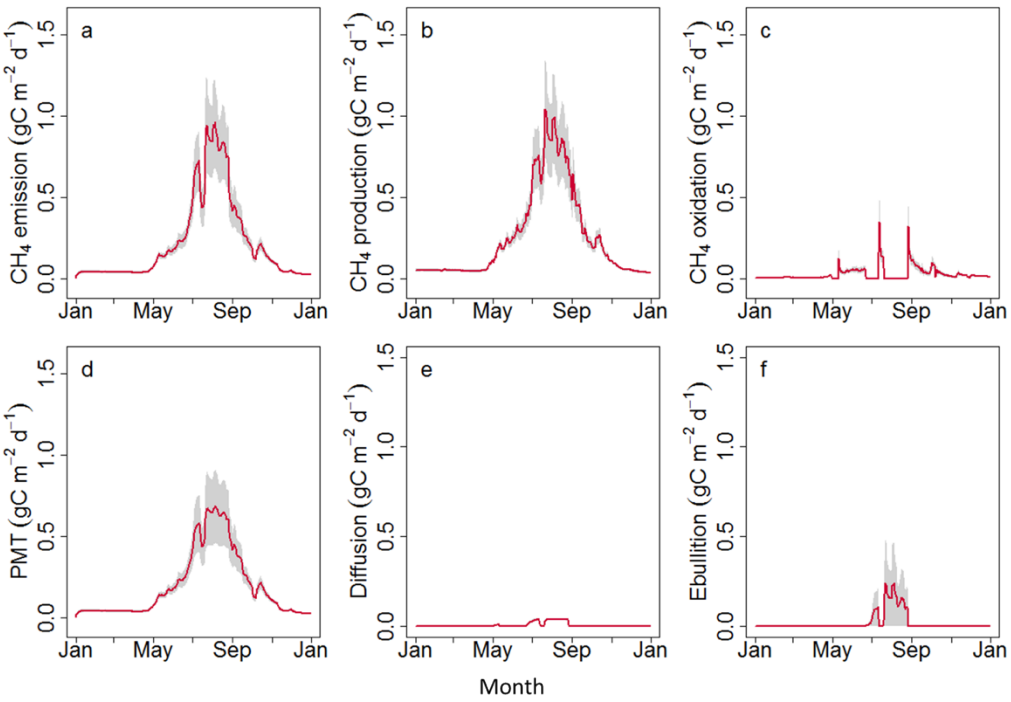

Figure 9. Simulated seasonal methane fluxes variation in 2011 under +9 °C warming condition. Red lines indicate CH_4 fluxes under +9 °C warming and 380 ppm CO_2. Shading areas correspond to mean ± one standard deviation based on 500 randomly chosen model simulations with parameters drawn from the posterior distribution.